Involvement of the fission yeast GATA transcription factor Gaf1 in TOR-dependent stress and nutrient responses

Olivia Hillson

A thesis submitted in partial fulfilment of the requirements of the University of East London for the degree of Masters of Research

School of Health Sport and Bioscience

September 2018

Abstract

The Target of Rapamycin (TOR) pathway is responsible for the growth and metabolic control of a cell, in response to nutrients and stress. This pathway, functioning through distinct protein complexes known as TORCs (TORC1 and TORC2 in yeasts and humans), is highly evolutionarily conserved. This allows for fission yeast, *S. pombe*, to serve as a model for humans in this study. Understanding genetic control of the TOR pathway is considered to have the potential to present pharmacological and dietary interventions for ageing and age-related diseases such as Alzheimer's and diabetes. In this study, the highly conserved GATA transcription factor Gaf1, orthologue of GATA6 in humans, is investigated for its role in TOR by studying phenotypical and transcriptional differences between *wild type* and *gaf1*Δ cells with and without TOR inhibition. The work makes use of microfermentation experiments to determine changes in growth kinetics as well as microarray data to understand gene expression changes that might underpin these phenotypes. The results highlight the need for further investigation in this area by suggesting a complex interplay between TORC1 and TORC2 and implicating Gaf1 in both spatial and temporal aspects of cell growth. The results support recent findings of Gaf1 involvement in ncRNA expression and tRNA binding, but suggest a more complicated involvement with organonitrogen metabolism and nitrogen catabolite repression.

Acknowledgements

Firstly, an overwhelming amount of thanks goes to my Director of Studies, Babis. He has been a never-ending source of encouragement, expert advice and support, without which I would never be where I am today. He has shown me that I am capable of much more than I thought, and I hope this thesis is testament to that. My time in the UEL labs during this research has not always been smooth sailing and I would like to thank my fellow PGRs for always being there to offer advice and support especially Suam Gonzalez. Extra-special thanks goes to my 'lab mum' Martina Neville for always being on my side and never letting me open the Virkon bucket without a mask on (my future lungs will thank you, too). I would also like to thank Prof. J Bähler and his lab at University College London, particularly Mimi Hoti, for their friendly welcome during my use of their facilities for this research.

I would like to thank all of my family and friends for their ongoing support and constant care. There will never be enough thanks for my Mum and Dad for always believing in me, funding this degree, and learning to care about yeast. I couldn't be here without them in all manner of ways. Special mention to my household for putting up with me when the work was making me more sociopathic than usual, particularly Emily for being a constant source of rational support and always making me tea even though I never make it for anyone else. I would like to send very special thanks to Yolanta Beinarovica for being the best kind of friend, reading everything I write and believing I was a good scientist when I couldn't manage it myself.

Last, but by no means least, I would like to give an honourable mention to Steven Green for genuinely wanting to read this thesis for the science.

Table of Figures

Abbreviations

Gaf1 – Protein transcription factor Gaf1

gaf1 – Gene encoding transcription factor Gaf1

*gaf1*Δ - *S.pombe* strain with *gaf1* deletion

wt – *Wild type* strain 972h-

TOR – Target of Rapamycin cellular pathway

TOR1 – Protein kinase integral to TORC2 in fission yeast

TOR2 – Protein kinase integral to TORC1 in fission yeast

TORC1 – One of the two distinct protein complexes in TOR in fission yeast

TORC2 – One of the two distinct protein complexes in TOR in fission yeast

YES – Nutrient rich media for fission yeast

EMM2 – Minimal nutrient media for fission yeast

Caf/rap – Combinational treatment with caffeine and rapamycin to inhibit TOR

KAN – resistance gene to the antibiotic G418 (geneticin)

NAT – resistance gene to the antibiotic nourseothricin

clonNAT – the antibiotic nourseothricin

DEPC water – diethyl pyrocarbonate water used to inactivate RNAse enzymes

GO – Gene ontology

ncRNA – Non-coding RNA

Contents

1 Chapter 1: Introduction

The Target of Rapamycin (TOR) pathway serves as a regulator of cellular metabolism and growth with regards to cell proliferation and survival (Laplante and Sabatini, 2009). To this effect, TOR inhibition leads to growth inhibition and lifespan extension in diverse experimental systems (Rallis et al., 2013). As the TOR pathway is highly conserved from yeast to man, research using genetically tractable organisms such as *Schizosaccharomyces pombe* (fission yeast) are useful and relevant models for mammalian and human TOR signalling pathways, and have the capacity to offer insights on physiological mechanisms and disease. In humans, there is a single TOR kinase while in fission yeast there are two, TOR1 and TOR2. The two TOR kinases exist within two structurally and functionally distinct protein complexes known as TOR complex 1 (TORC1) and TOR complex 2 (TORC2) (Loewith and Hall, 2011). TORC1 positively regulates growth and supresses cellular responses to nitrogen stress in the presence of a preferred nitrogen source while TORC2 is less well defined and is implicated in cell survival and proliferation, DNA metabolism and damage (Rallis et al., 2013). The following paragraphs introduce the TOR pathway in metabolism, growth and disease and the relationships of the GATA transcription factor Gaf1 with the pathway.

1.1 Discovery of TOR Kinases

TOR was initially discovered, as its name suggests, as the target pathway for the drug rapamycin. Rapamycin was first isolated from the bacterium *Streptomyces hygroscorpicus* by Suren Sehgal in 1972 and identified as an antifungal (Vezina et al., 1975). Upon further analysis rapamycin showed potential as an immunosuppressive drug and gained FDA approval for this purpose (Blenis, 2017). Initial discovery of the TOR pathway came much later in the early 1990s by several methods. Initially a genetic screen for *Saccharomyces cerevisiae* mutants identified the gene encoding the cellular receptor for rapamycin, FKPB (*FPR1*) (Heitman et al., 1991a) after the same team had previously identified FKPB as the binding protein for rapamycin's structural homologue FK-506 (Heitman et al., 1991b). While the genes were identified in Heitman's 1991 screen, TOR1 and TOR2, the two TOR kinase

homologues more commonly referred to as the targets of Rapamycin, were not fully characterised until 1993 and 1994 when TOR2 was identified as a target of rapamycin (Kunz et al., 1993) and TOR1/2 were found to be structurally and functionally similar but non-identical (Helliwell et al., 1994).

1.2 Evolutionary Conservation of TOR kinases and TOR complexes

The importance of these characterisations can only be fully appreciated when viewed within the context of the conservation of TOR from yeast to man. Rather than the two homologues found in yeast (Shertz et al., 2010), in humans TOR exists as only one kinase known as mechanistic TOR or mTOR (Laplante and Sabatini, 2009). The isolation of mTOR came in 1994 and marked the first evidence that yeast could be used as a viable model organism for TOR in humans. mTOR was initially identified as the FKBP-rapamycin-associated-protein (FRAP) (Brown et al., 1994) but was referred to as mTOR after it was found to be an orthologue to the yeast TOR homologues (Abraham, 1998). The existence of mTOR prompted research which established that mTOR functions as in yeast within two highly conserved protein complexes termed mTORC1 and mTORC2 as shown in figure 1 (Blenis, 2017) .

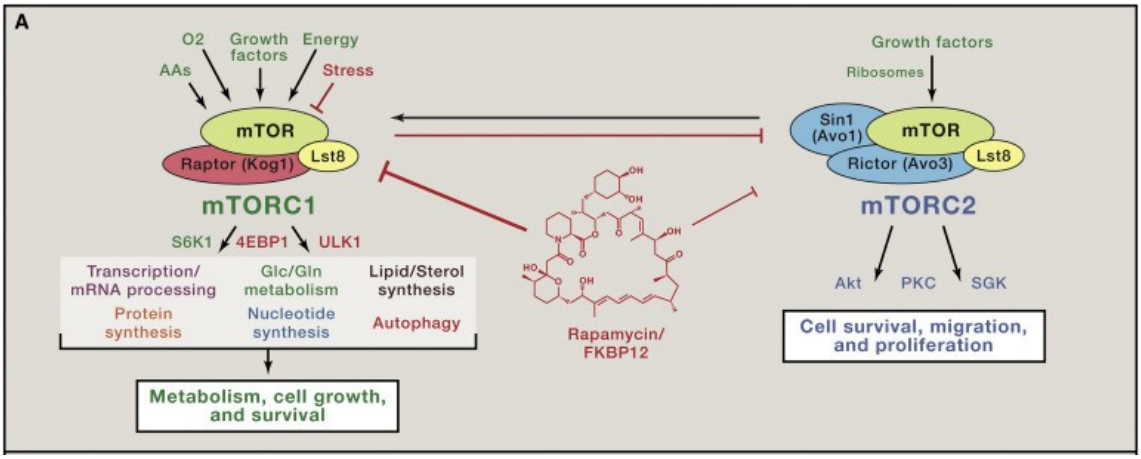

Figure 1: mTORC1/2 complexes and implication in diverse cellular processes and rapamycin inhibition of both mTOR complexes. The figure highlights that the role of mTORC1 is much more clearly defined than that of mTORC2 (Blenis, 2017)

In all known TOR incarnations, the targets of rapamycin, TOR kinases combine with other proteins to create TORC1 and TORC2 as exemplified by figures 1 and 2. The distinction between TOR1/2 and TORC1/2 is an important one when understanding the finer details of the pathway.

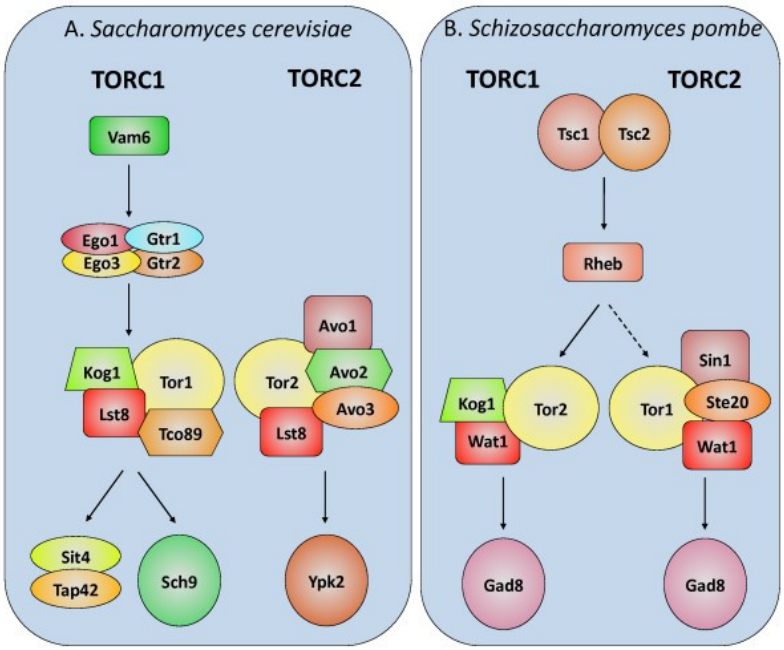

Figure 2: TORC1/2 in S.cerevisiae and S.pombe where functional homologues between the species are shown by matching shape and colour. In S.cerevisiae the TOR kinases are involved in the opposite TOR complexes than in S.pombe. (Shertz et al., 2010)

The two complexes were believed to be distinct due to research suggesting distinct functions and different subcellular localisations (Loewith and Hall, 2011) however more recent studies have suggested a much more complex interplay between them (Gonzalez and Rallis, 2017) with functions traditionally linked to TORC1 being mediated by TORC2 and vice versa.

1.3 Emerging functions of TORC1/2

TORC1 and TORC2 have, for many years, been linked to very separate cellular functions. TORC1 has mostly been linked with temporal aspects of cell size and growth and TORC2 with spatial growth. As research has progressed,

exceptions to these assumed roles continued to emerge, until they became too numerous to ignore. Recently there has been an acceptance that this separation of complex function is too constricting for the reality of TOR's nature (Gonzalez and Rallis, 2017). Some such exceptions to assumed roles are: the involvement of TORC1 in the actin cytoskeleton (Aronova et al., 2007) and the involvement of TORC2 in the timing of cell division in fission yeast (Gonzalez and Rallis, 2017).

To investigate these emerging roles of each complex individually, mutant strains can be produced where either TORC1 or TORC2 is no longer functional. For TORC2 the kinase itself, TOR1, can be removed by disruption or deletion of the *tor1* gene. In respect to TORC1, TOR2 is an essential gene and disruption or deletion of this gene does not yield viable cells (Weisman and Choder, 2001). This means that TORC1 needs to be functionally disrupted by deletion of another TORC1 component gene such as *tco89* (Nishida and Silver, 2012).

1.4 TOR in Disease

TOR inhibition has been implicated in human disease since before it was even defined, with the use of Rapamycin and FK506 as immunosuppressant drugs (Blenis, 2017). More recently TOR has been of interest in cancer research, mTOR has been shown to be involved in multiple cancers and dysregulation of TOR has been implicated in familial cancer syndromes (Beauchamp and Platanias, 2013). TORC1/2 inhibition has been shown to decrease the survival of some triple negative breast cancer (TNBC) cells *in vitro* and *in vivo,* but some subsets of cancer cell, such as cancer stem cells, (CSCs) are resistant to this leading to interest into this resistance mechanism as a drug target (Bhola et al., 2016).

From a wider perspective TOR is heavily implicated in several diseases, especially those related to ageing. It has suggested involvement in diabetes, Alzheimer's, and hepatic steatosis to name a few (Dazert and Hall, 2011). Given the global role of TOR within the cell, it follows that impacts of its dysregulation would be widespread. Arguably, some of the most interesting research is the involvement of mTOR in neurodegenerative diseases. Here its involvement is due to TOR's role in autophagy which can be used to clear

accumulated misfolded proteins, a common pathology among these diseases. Rapamycin has been utilised in some trials to use this as a treatment target (Dazert and Hall, 2011). This research is particularly encouraging as it presents an overarching approach for a few diseases that doesn't require further knowledge of the poorly understood mechanisms which cause them. However, it does reinforce how widespread the negative implications of TOR dysregulation could be. The conservation of TOR from yeast to man, and its direct implications on a plethora of diseases, opens the door to research into TOR as a drug target using diverse approaches and models.

1.5 TOR Inhibition

mTOR's existence in two protein complexes results in interesting effects during inhibition by rapamycin. The two complexes, mTORC1 and mTORC2, are differently affected by rapamycin treatment with mTORC1 inhibition occurring immediately and mTORC2 inhibition occurring only after prolonged treatment with the drug (Schreiber et al., 2015). The two mTOR complexes are not only structurally different from one another, they also have distinct differences in their downstream functions. mTORC1 is associated with the control of anabolic and catabolic processes in response to nutrient availability (Johnson et al., 2013) and is much better understood than mTORC2, but it is believed that both could potentially affect healthy lifespan and ageing. This makes rapamycin an interesting potential drug as it could be used to affect mTORC1 alone or both mTORC1 and mTORC2.

As TOR's name suggests, rapamycin and its analogues or 'rapalogs' were the first inhibitors of the pathway/kinase to be used. They have long been considered a key candidate for the pharmacological intervention of ageing, with evidence showing that rapamycin increases the lifespan and health-span in mouse models having been successfully reproduced (Johnson and Kaeberlein, 2016). In fission yeast, rapamycin inhibition of TOR is aided by the addition of caffeine (Rallis et al., 2013). Caffeine itself is a TORC1 inhibitor (Wanke et al., 2008) and the combinational treatment with caffeine and rapamycin has a greater effect than the individual treatments (Rallis et al., 2013). Rapalogs hold an advantage over rapamycin itself as a treatment option, as they can be

developed to have more favourable pharmacological kinetics and specificity, and provide an opportunity for intellectual property which can be advantageous to the drug development industry (Xie et al., 2016).

Increasing research into the success of mTOR inhibition led to not only the synthesis of rapalogs but also the synthesis of other, potentially more effective, mTOR inhibitors. Developed by AstraZeneca, the ATP-competitive mTOR inhibitors Torin1 (Thoreen et al., 2009) and subsequent Torin2 (Liu et al., 2013), are two such examples. These drugs, can inhibit both mTORC1 and mTORC2 through the direct inhibition of the mTOR kinase (Xie et al., 2016). Torin1 has been used in a few settings to demonstrate anti-ageing properties. In 2015, Torin1 was shown to be more potent than rapamycin when inhibiting senescent morphology in human cells suggesting that these processes may rely on rapamycin insensitive components of TOR and presenting the drug potential of this class of mTOR inhibitors (Leontieva and Blagosklonny, 2016, Leontieva et al., 2015) . Very recently, dietary introduction of Torin1 has been shown to increase lifespan in *Drosophila melanogaster* without reducing fertility (Mason et al., 2018) showing potential for this drug to increase lifespan without reducing life quality.

1.6 Gaf1 and TOR

Much of the research into TOR itself is now focussed on using diverse genetic approaches. This presents further understanding of TOR and identifies targets for its control. Gaf1 is a GATA transcription factor, of 91.78 kDa in size, involved in the TOR pathway in fission yeast. It has been shown to be evolutionarily conserved with a known orthologue in humans, GATA6 (PomBase). GATA6 is a zinc finger domain containing, highly conserved GATA transcription factor (Suzuki et al., 1996) with known homologues in both mice and rats (HUGO Gene Nomenclature Committee).

TORC1 has been shown to positively regulate the phosphorylation of Gaf1 causing it to remain in the cytoplasm. When the cell encounters nitrogen stress TORC1 is inhibited and Gaf1 is dephosphorylated by PP2A-like phosphatase Ppe1. This allows it to enter the nucleus where it positively regulates *isp7* and negatively regulates *ste11* (Laor et al., 2015).

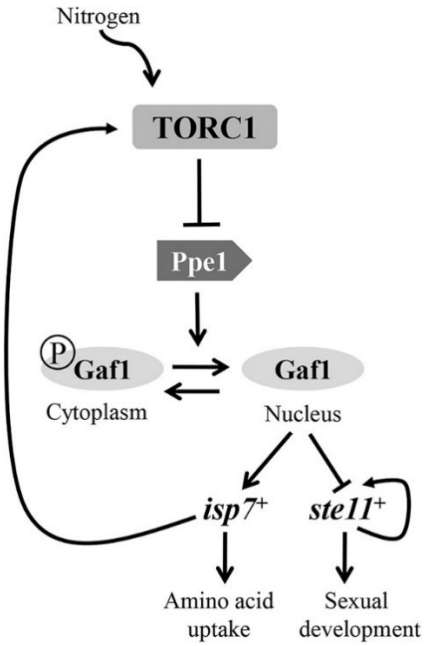

Figure 3: TORC1 negative regulation of Gaf1 localisation. TORC1 inhibits the dephosphorylation of Gaf1 causing it to remain in the cytoplasm. When the cell encounters nitrogen stress Gaf1 is dephosphorylated and enters the nucleus where it positively stimulates isp7 which in turn stimulates TORC1. (Laor et al., 2015)

The gene *isp7* encodes for the oxygenase Isp7 which controls amino acid uptake by regulating the transcription of amino acid permeases. In response to nitrogen stress Gaf1 is no longer inhibited by TORC1 and *isp7* is upregulated, allowing amino acid uptake to remain the same (Laor et al., 2014). The *ste11* gene codes for the transcription factor Ste11 responsible for positively regulating genes required for the initiation of meiosis. *ste11Δ* mutants have been shown to be completely defective in mating and sporulation whereas the overexpression of *ste11* leads to sexual reproduction, even in stress conditions (Kim et al., 2012). This suggests that Gaf1 is responsible for the decrease in sexual reproduction during nitrogen stress.

Currently, knowledge of TOR is making rapid strides from many different angles, quite possibly due to research spurred on by new interest in TOR as a drug target. The roles of Gaf1, as it stands, are only very partially understood, but the recent relevant discoveries create an interesting niche in understanding TOR-related nutrient and stress cellular responses. In addition, research on TOR has focused on the upstream players regulating its complexes and its direct kinase targets. Nevertheless, understanding of factors affecting TOR-

dependent transcriptional regulation has been limited. Early data from microarray analyses and ChiP-seq indicate that Gaf1 mediates transcriptional effects downstream of TOR related to metabolism, cellular growth and ageing (Rallis unpublished data-personal communication).

The aim of the present research is to understand the functions of Gaf1 in TOR-related signalling and cellular events. with regards to specific involvement in TORC1/2 by cellular growth and transcriptome analysis upon TOR inhibition. The work makes use of the differences in inhibition between caffeine and rapamycin and Torin1, and spatial and temporal growth measures to enrich knowledge of TORC1/2 involvement. Developing a deeper understanding of these cellular processes could have far-reaching, knock on effects to pharmacological and dietary interventions for ageing and age-related diseases.

2 Chapter 2: Materials and Methods

2.1 Materials

2.1.1 Fission yeast strains

Table 1: Table of fission yeast strains and strain names used in thesis text

Name used in text	Strain name
Wild type (*wt*)	*972h-*
*gaf1*Δ	*gaf1Δ::kanMX6 h-*
*tco89*Δ	*tco89Δ::kanMX6 h+*
*tor1*Δ	*tor1Δ::kanMX6 h+*

2.1.2 Media

Table 2: Details of media, stressors and antibiotics

Material	Details
YES broth/agar	Formedium YES Broth For solid media 16g/l agar was added
Minimal broth	Formedium EMM broth without nitrogen NH_4Cl added
Torin1	Tocris, Cat. No. 4247
Caffeine	Sigma Cat. No. C0750-500G
Rapamycin	LC laboratories Cat. No. R-5000
Arginine	Sigma Cat. No. A5006-100G
clonNAT (nourseothricin)	Werner Bioagents Cat. No. 5
G418 (Geneticin)	Thermofisher Cat. No. 11811023

2.1.3 Primers

Primers were designed using Pombe PCR Primer Programs from Bahler Lab Resources (BählerLab) and ordered from Eurofins (EurofinsGenomics, 2019).

Description	Sequence
MX4/6cass up	5′GACATGGAGGCCCAGAATAC3′
MX4/6cass down	5′TGGATGGCGGCGTTAGTATC3′

Gaf1 deletion forward	5'ATTTCATTCGTTTATTTTTTGTTTCGGTTTTTTATT CGGAAACTTCCCTTTTTCTTTCTTATCCACATTTCAAG CTGGCTCGGATCCCCGGGTTAATTAA3'
Gaf1 deletion reverse	5'TGCACACGTAAGCCTCTTGCTCATACAATTAATCGA CTTTTCCGACAAGAAAAAAATTCAAGTCGAAAATATA CTATCTAGAATTCGAGCTCGTTTAAAC3'

2.2 Methods

2.2.1 Library Screening

The Bioneer fission yeast library version 5 (Bioneer, 2010) was grown on YES agar at 32˚C and 10uM Torin1 YES agar plates were prepared. The library was spotted onto Torin1 agar plates using a Singer ROTOR machine and incubated at 32˚C for four days. Plates were photographed and processed into gridded images using the R package Gitter (Wagih and Parts, 2014) for computational comparison of colony size. The list of mutants with a colony size ratio of >3 and <100 was used for gene ontology analysis using AnGeLi (BählerLab, 2015) online software. GO biological processes which showed a greater than twofold change from the background frequency were used for analysis. The online PInt protein prediction tool (BählerLab) was used to predict proteins interacting with Gaf1 and these proteins were then compared to the list of resistant genes to identify future targets for research.

2.2.2 Microfermentation

Microfermentation was carried out using the m2p labs Biolector to read biomass over a 48hour time course. 20ml YES precultures were grown overnight at 32˚C to OD600~0.2 and then 1.5ml of culture was transferred to each flower plate well. The cultures were treated with stressors once in the plate and the microfermentation began immediately following this. Analysis was conducted using the BioLection program, the R package grofit, and in-house R scripts for normalisation.

2.2.3 Cell Size Microscopy

A *wild type* YES culture was grown overnight at 32˚C to OD600=0.2 and split into two. One culture was then treated with 20nM Torin1. Untreated and treated cells were then stained with calcuofluor and septated cell lengths of 50 cells at each timepoint were calculated using Volocity Program. Quantitative statistical analysis of cell length data was performed using prism (GraphPadSoftware, 2018). Turkey's multiple comparisons test was chosen for statistical analysis to compare the mean of all timepoints to all others.

2.2.4 Microarray Analysis

Microarrays were carried out using YES *wt* and *gaf1Δ* cell cultures grown to OD600= 0.5 and each of these replicated and treated with 10mM caffeine/100ng/ml rapamycin or 20nM Torin1 for 1 hour. The twelve cultures used in the microarrays are shown in the table below:

Table 3: Details of cultures used in microarray experiment

Repeat	Strain	Treatment
1	*Wild type*	None
1	*Wild type*	10mM caffeine/100ng/ml rapamycin
1	*Wild type*	20nM Torin1
1	*gaf1Δ*	None
1	*gaf1Δ*	10mM caffeine/100ng/ml rapamycin
1	*gaf1Δ*	20nM Torin1
2	*Wild type*	None
2	*Wild type*	10mM caffeine/100ng/ml rapamycin
2	*Wild type*	20nM Torin1
2	*gaf1Δ*	None
2	*gaf1Δ*	10mM caffeine/100ng/ml rapamycin
2	*gaf1Δ*	20nM Torin1

Cells were harvested at OD 600 ~0.2 and volumes were adjusted according to OD. The cells were centrifuged for 2min at 2000rpm and the supernatant was discarded. Cell pellets were snap frozen using liquid nitrogen and stored at

70˚C. Cells were thawed on ice and pellets were resuspended in 1ml of DEPC water, spun for 10 seconds at 5000rpm and the supernatant was discarded. 750µl of TES was used to resuspend each pellet and 750µl of acidic phenol-chloroform (Sigma P-1944) was added, the tubes were vortexed and incubated at 65˚C in a heat block. Samples were incubated for 1 hour with vortexing for 10 seconds every 10 minutes. Samples were placed on ice for 1 minute, vortexed for 20 seconds and then centrifuged for 15 minutes at 20,000rcf, 4˚C. 2ml Qiagen phase-lock tubes were pre-spun for 10 seconds and 700µl of chloroform:isoamyl alcohol (24:1) (Sigma C-0549) was added to each tube. 700ul of the water phase from the samples was added to the phase-lock tubes and they were mixed thoroughly by inverting. They were then centrifuged for 5 minutes at 20,000rcf, 4˚C. 2ml Eppendorf tubes were prepared for each sample containing 1.5ml of 100% EtOH and 50µl of 3M NaAc pH 5.2. 500µl of the water-phase from each sample was transferred into these. The samples were vortexed for 10 seconds and stored at -20˚C overnight to precipitate.

Samples were centrifuged for 10 minutes at 20,000 rcf at room temperature and the supernatant was discarded. 500µl of 70%EtOH (4˚C, made with DEPC water) was added and the samples were spun for a further 1 minute with the same tube orientation. The supernatant was discarded, and the pellets were spun for a further 5 seconds and any remaining supernatant was removed before the pellets were air dried for 5 minutes at room temperature. 100µl of DEPC water was added to resuspend the pellet (by pipetting and 10 sec vortex) and the samples were incubated at 65˚C for 1 minute. RNA concentration was measured using a Nanodrop and volumes corrected to use 100µg of RNA for purification. 3 volumes of 100% EtOH was added to excess RNA sample these were stored at -70˚C. Purification was carried out using RNeasy mini spin columns (Qiagen) as per the manufacturer's instructions and the columns were eluted twice with RNase-free water. The final RNA concentration was measured by Nanodrop and these concentrations were then adjusted to 2µg/µl.

After RNA extraction the microarray experiment was set up to include a pool system to allow all microarrays to be compared to each other and a dye swap between repeats to account for dye bias. This is shown in figure 4.

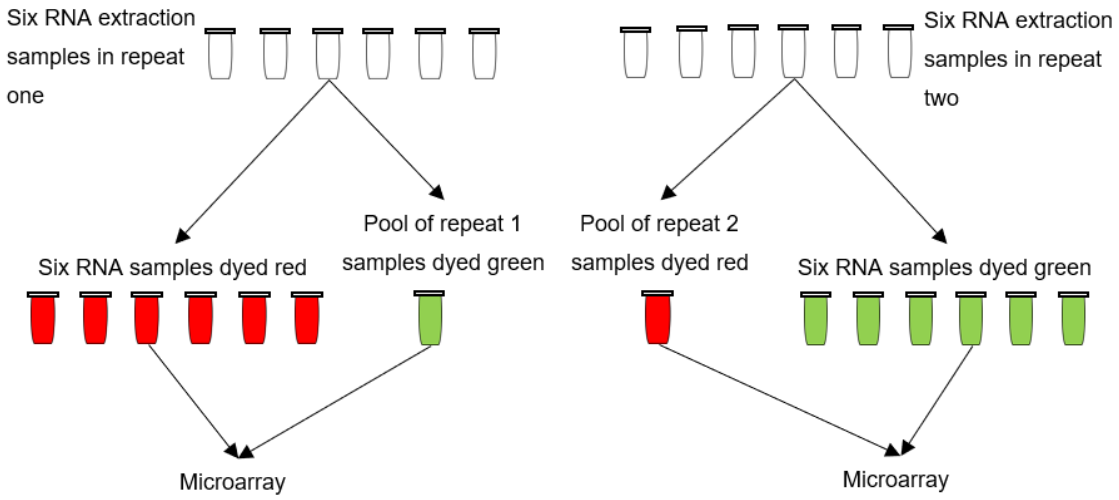

Figure 4: Diagram to show process of pool and dye swap strategy for RNA samples used in microarray analysis experiment.

Agilent 8 × 15K custom-made *S.pombe* expression microarrays were used, and hybridizations and subsequent washes performed according to the manufacturer's protocols. The obtained data were scanned and extracted using GenePix, processed using R scripts for quality control and normalization, and analyzed using GeneSpring GX3 (Agilent Technologies UK Ltd, Wokingham, UK). Two independent biological repeats with a dye swap were performed. Online bioinformatics tools and R scripts were used to analyse gene lists and GO enrichment was performed using the AnGeLi bioinformatics tool available online (BählerLab, 2015).

2.2.5 Production of gaf1Δ::natMX6 strain from gaf1Δ::kanMX6

DNA for transformation was prepared by PCR of a plasmid containing NAT Gaf1 knockout construct using the primers stated below:

MX4/6cassUP: 5′-GACATGGAGGCCCAGAATAC-3′

MX4/6cassDwn: 5′-TGGATGGCGGCGTTAGTATC-3′

PCR product DNA fragments were separated by gel electrophoresis on 1% agarose gels for one hour and visualised under u/v light by staining with SYBR-Safe.

gaf1Δ::kanMX6 strain yeast were grown overnight in EMM media to OD 0.2-0.5. These cultures were then centrifuged and the cells washed with sterile water once before being resuspended in 1ml of sterile water. The cells were then centrifuged again and washed in 1ml LiAc-TE, centrifuged a final time and resuspended in 100ul of LiAc-TE. 5ul of DNA was added to the 100ul of cells and this was incubated on the bench for 10 minutes. 260ul of LiAc-TE-40%PEG was then added and the cells were incubated at 30˚C in a shaking incubator for 60 minutes. After the incubation 43ul of prewarmed DMSO was added and the cells were heat shocked for 5 minutes at 43˚C. Cells were then centrifuged, washed with sterile water and then resuspended in 750ul of sterile water for plating on three YES agar plates. Once these plates were grown at 30˚C for ~24-48hours they were replica plated on to YES clonNAT plates for selection. Any transformants were streak plated on to YES G418 and YES clonNAT plates to check for the absence of a KAN resistance gene and the presence of a NAT resistance gene.

After the above method proved unsuccessful several alterations were made to the methodology one by one to improve transformation efficacy. Adaptations tested are shown in the table below:

Table 4: Details of method alterations

Original	**Alteration**
5ul of DNA added	10ul of DNA added
20ml of overnight culture used	40ml of overnight culture used.
Cells plated on YES immediately	Cells left in 750ul of EMM media overnight on the bench before YES plating
Cells incubated for 60 minutes	Cells incubated for 2 hours
Cells incubated for 60 minutes	Cells incubated for 3 hours
Cells grown in EMM media	Cells grown in YES media
Cells plated on YES immediately	Cells left in 750ul YES media overnight in the 30˚C incubator before YES plating

Cells plated on YES immediately then replica plated onto YES clonNAT agar	Cells left in 750ul YES media overnight in the 30˚C incubator before plating directly onto YES clonNAT agar
Cells plated on YES immediately then replica plated onto YES clonNAT agar	Cells left in 10ml YES media overnight in in the 30˚C incubator before gently spinning down, removal of excess media and plating directly onto YES clonNAT agar.
Cells incubated for 60 minutes in 30˚C shaking incubator	Cells incubated for 60 minutes in 30˚C stationary incubator
Older DNA synthesised by PCR	New DNA synthesised using PCR
PCR product used directly without clean-up	PCR product cleaned up using QUIAGEN PCR Clean Up Kit

2.2.6 Production of gaf1::natMX6 strain from Wild Type strain

DNA for transformation was produced by PCR from a plasmid containing NATMX6 cassette flanked by *gaf1* homology regions. The PCR product containing the antibiotic resistance/deletion cassette was generated using the primers stated below:

Gaf1DF: 5'- ATT TCA TTC GTT TAT TTT TTG TTT CGG TTT TTT ATT CGG AAA CTT CCC TTT TTC TTT CTT ATC CAC ATT TCA AGC TGG CTC GGA TCC CCG GGT TAA TTA A- 3'

Gaf1DR: 5'- TGC ACA CGT AAG CCT CTT GCT CAT ACA ATT AAT CGA CTT TTC CGA CAA GAA AAA AAT TCA AGT CGA AAA TAT ACT ATC TAG AAT TCG AGC TCG TTT AAA C- 3'

PCR product DNA fragments were separated by gel electrophoresis on 1% agarose gels for one hour and visualised using SYBR-Safe.

Wild type fission yeast was grown overnight in YES media to OD 0.2-0.5. The cultures were then centrifuged and washed with sterile water once. Following centrifugation cells were resuspended in 1ml of sterile water. The cells were then centrifuged and washed in 1ml LiAc-TE, before being centrifuged a final time and then resuspended in 100ul of LiAc-TE. 5ul of DNA was added to the

100ul of cells and this was incubated on the bench for 10 minutes. 260ul of LiAc-TE-40%PEG was then added, and the cells were incubated at 30˚C in a static incubator for 60 minutes. After the incubation 43ul of prewarmed DMSO was added and the cells were heat shocked for 5 minutes at 43˚C. Cells were then centrifuged, washed with sterile water, and then resuspended in 750ul of YES and incubated at 30˚C overnight. These cells were then plated on to YES clonNAT plates for selection.

3 Chapter 3: Results

The techniques and approaches used in this investigation were specially chosen to develop a well-rounded view of Gaf1 involvement in TOR in fission yeast from both a phenotypical and transcriptomic standpoint. A genome wide screen for Torin1 resistance was used to demonstrate the *gaf1*Δ phenotype and identify mutants with a similar phenotype. Growth kinetics analysis was used along with cell size microscopy to further develop understanding and identify features of this phenotype of long life in TOR inhibition. Transcriptomics in the form of microarrays identified some potential expression changes responsible for the phenotypes observed in the previous experiments.

3.1 A Genome-wide screen for mutants resistant to Torin1

A genome-wide Torin1-resistance screen using the version 5 Bioneer fission yeast deletion library covering 3,400 haploid deletion mutants with a 95.3% genome coverage (Bioneer, 2010) was performed to identify deletion mutants resistant to Torin1 growth inhibition. *gaf1Δ* was one of the strains identified to be resistant. Mutants showed differences in growth between control YES plates and Torin1 YES 10uM Torin1 plates (figure 5A and 5B). Plates were photographed and then colonies were quantified using the Gitter software (Wagih and Parts, 2014). An example of the photographed plates is shown in figure 5A and 5B and the processed quantified images in figure 5C and 5D. Firstly all colonies were normalised with the median of each plate to correct for differential growth between plates. The size ratio between the control and Torin1 plate colony size was then taken for each knockout strain to generate a ratio. From these ratios a gene list is created including all knockout mutants where the colony size ratio is >3 and <100 to be used for gene ontology (GO) enrichment; these arbitrary cut-offs are used to reduce the influence of outliers in the screen data on the GO analysis.

The results of the GO analysis which showed >twofold changed frequency to that of the background are shown in figure 6, a >twofold cut-off was used to identify the gene functions which were most disproportionately seen in the gene list as opposed to the background genome frequency. Figure 6 shows that most

of the resistant mutants are related to the endosome, vacuole and vesicular transport.

This study's Torin1 resistant knockout gene of interest, *gaf1*, has been shown to be resistant to Torin1 in previous screens (Lie et al., 2018) and was also shown here to be resistant with a library screen ratio of 8.79. PInt protein interaction analysis for Gaf1 is shown in figure 6. Here, line thickness denotes the confidence of the prediction and known interactions in *S.cerevisiae* are shown in red. Two genes were found to be both in the PInt predictions and as Torin1 resistant with a colony size ratio of >3 and <100. These can be found highlighted in yellow in figure 7 and detailed in table 5 along with GO biological processes for these genes.

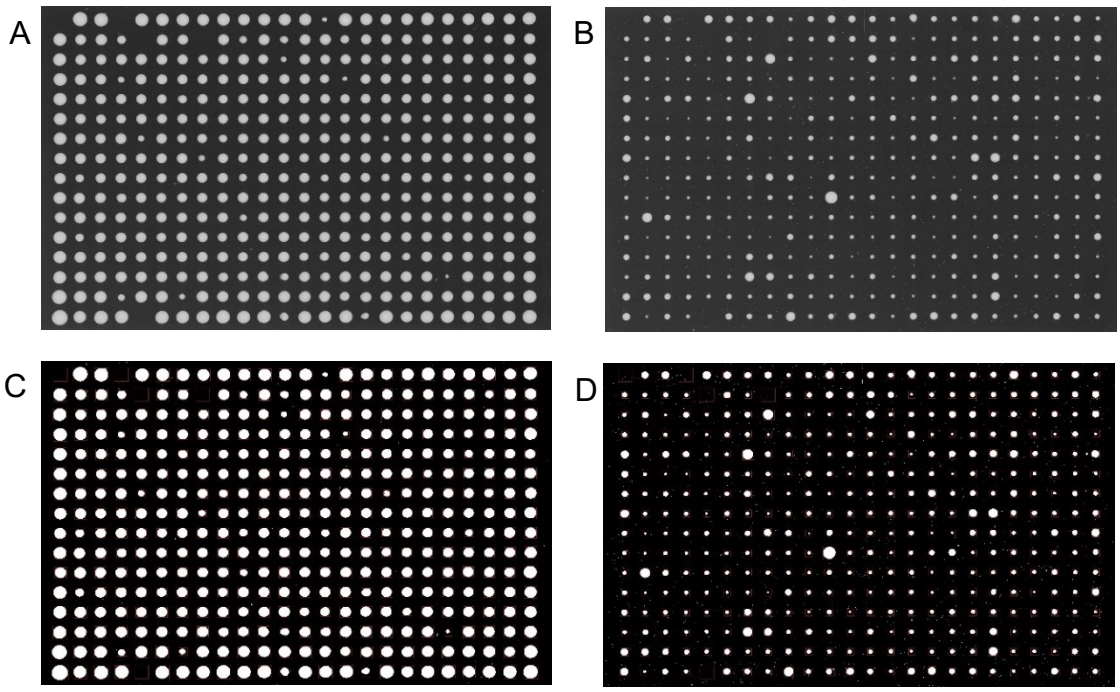

Figure 5: Example of image processing step for library screen data. Images A-D show the first control and Torin1 plates: (A) photograph of plate 'Control 1-4' (B) photograph of plate 'Torin1 1-4' (C) quantified image of plate 'Control 1-4' (D) quantified image of plate 'Torin1 1-4'. This image processing is repeated for the remaining control and Torin1 library plates before quantification using the R package Gitter (Wagih and Parts, 2014) to produce a table of strains and colony size ratios.

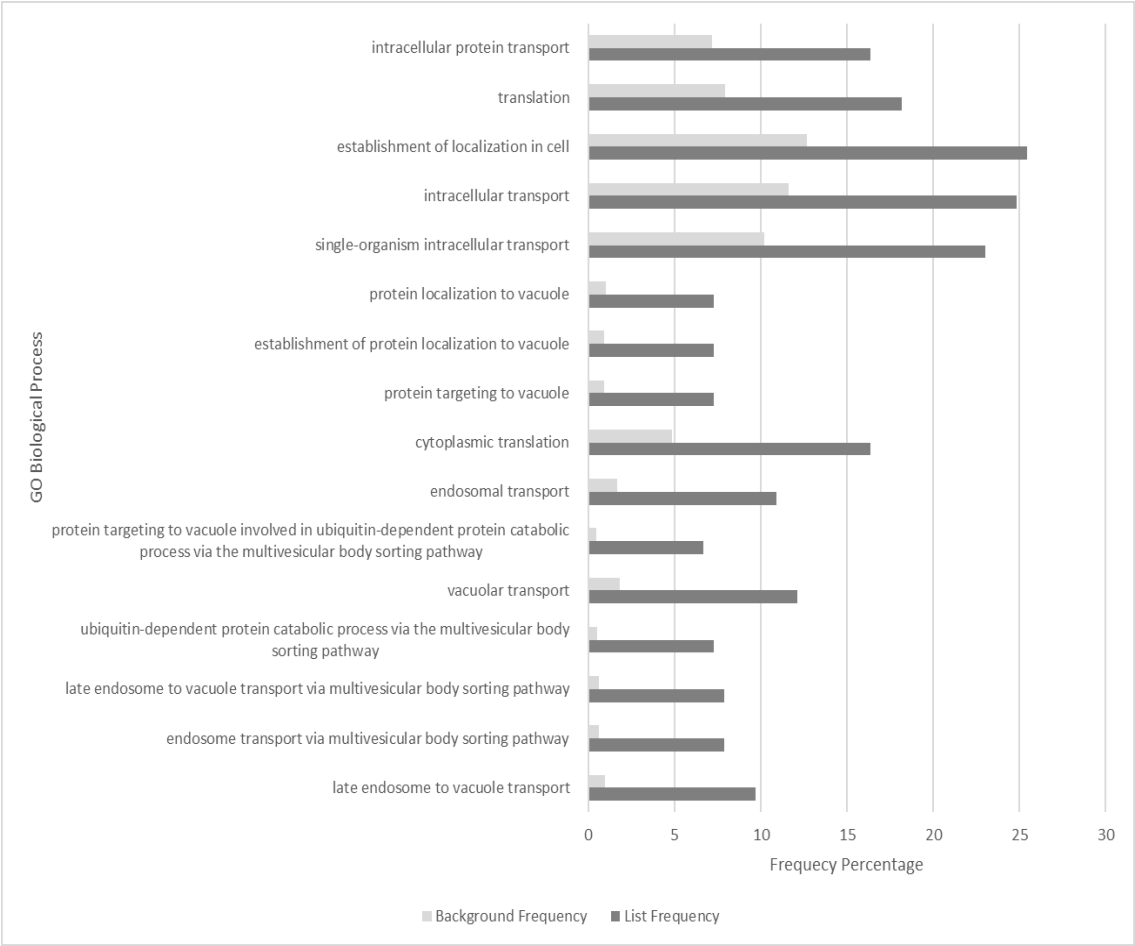

Figure 6: GO functions shown have a >twofold changed frequency in the Torin1 resistant gene list compared to the background genome frequency produced using AnGeLi (BählerLab, 2015). Endosome, vacuole and vesicle transport are particularly highlighted as common functions among genes resistant to Torin1 inhibition.

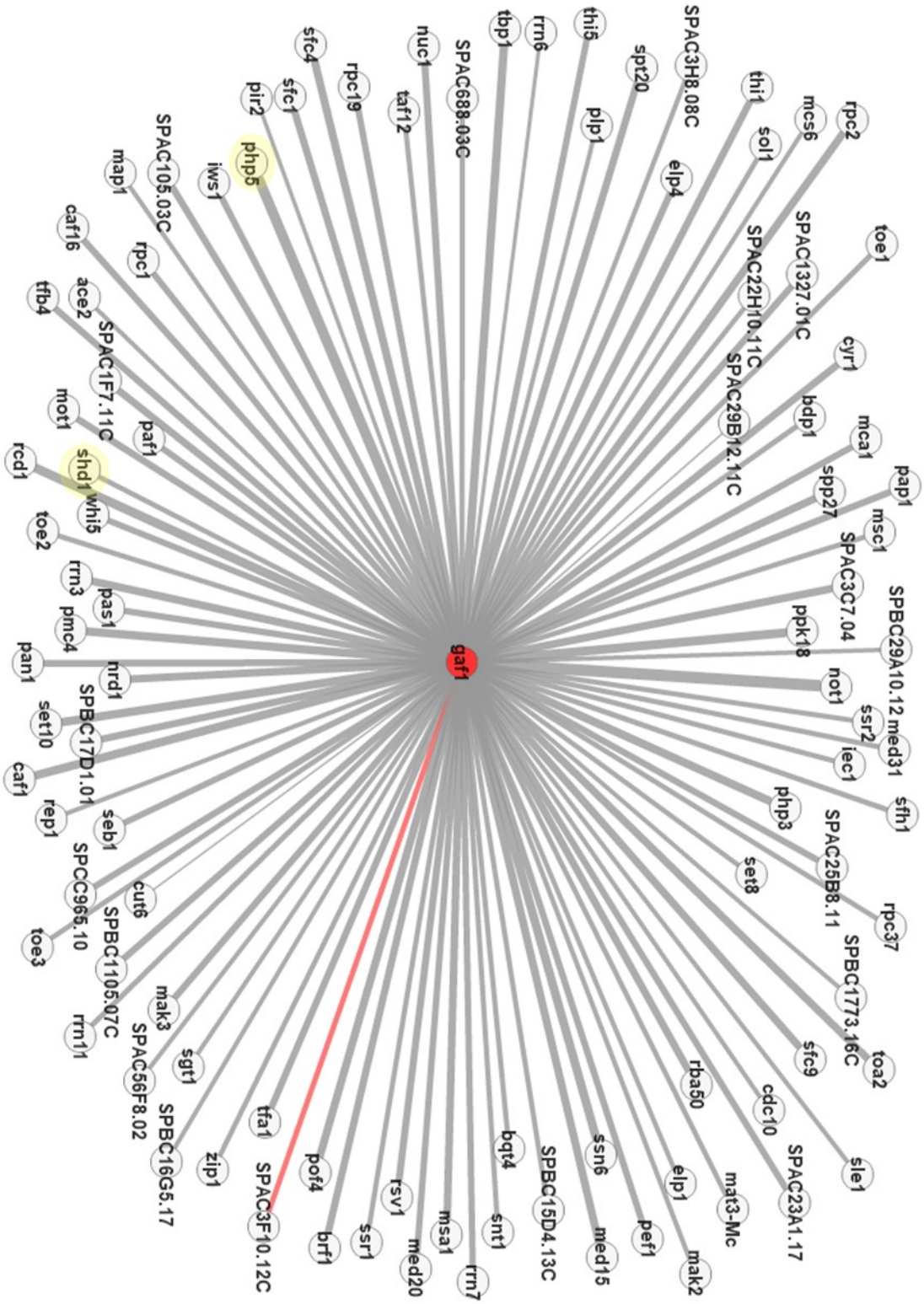

Figure 7: Diagram of PInt protein interaction predictions for gaf1 (BählerLab) where line thickness represents confidence in prediction, red lines represent known interactions from BioGRID, and genes which also showed resistance to Torin1 treatment in the screen are highlighted in yellow.

Table 5: Genes identified by both the Torin1 library screen and the PInt Interaction prediction for gaf1. PInt Interaction prediction tool uses two machine learning algorithms, Support Vector Machine (SVM) and Random Forest (RF). Using the two combined returns fewer but more confident predictions (BählerLab).

Gene ID	***Gene name***	***Library screen ratio***	***SVM Score***	***RF Score***	***GO Biological process***
SPAC16E8.01	*shd1*	3.389796882	0.783875	0.612	Actin cytoskeleton organisation and vesicle mediated transport.
SPBC3B8.02	*php5*	3.055288347	0.873156	0.702	Regulation of transcription by RNA polymerase II.

Of the two genes found to be in both the library screen gene list and also the PInt prediction gene list. *php5* was also identified as resistant to Torin1 in a previous screen (Lie et al., 2018). The GO enrichment can be used to develop an understanding of which biological processes allow interaction between *gaf1* and the identified genes.

3.2 Growth kinetics analysis of gaf1Δ mutant using microfermentation

Once *gaf1*Δ had been identified as resistant to Torin1 by both the previous published library screen (Lie et al., 2018) and the screen carried out in this work, a more comprehensive analysis of cellular growth changes was required. The library screen implicated Gaf1 in TOR signalling so microfermentation was used to further investigate any differences in growth kinetics as well as quantify the growth of *gaf1*Δ in the presence of Torin1.

Microfermentation analysis and quantification of lag phase using a modified R script based on the grofit package (Kschischo, 2010) (figure 9B) of *wild type* and *gaf1*Δ strains showed that *gaf1*Δ has a shorter lag phase compared to *wild-type* when treated with 15mM of Torin1, while the untreated cultures displayed identical growth kinetics and reached stationary phase simultaneously (Figure 8). To further investigate the behaviour of *wild-type* and *gaf1*Δ cells we undertook experiments in which Torin1-treated cultures were supplemented with arginine, a TOR stimulator (Yuan et al., 2015). Addition of arginine to the cultures could lead to counteraction and reversion of the effects of Torin1 inhibition. *Wild type* cells showed a decrease (rescued) lag phase where *gaf1*Δ cells did not. *tor1*Δ and *tco89*Δ (*tco89*Δ being a core component of fission yeast TORC1) cells were also tested, and both showed rescued lag phases with the addition of arginine (figure 9).

All Torin1 treated cultures displayed a signature decrease in biomass immediately and until ~hour 5. This decrease in biomass was present even in *gaf1*Δ cells and was rescued by the addition of arginine in both *wild type* and *gaf1*Δ cells (figure 10). Increasing concentrations of arginine caused an unexpected increase in lag phase length (figure 11A). This correlated directly with the increasing pH found by increasing concentrations of arginine (figure 11B).

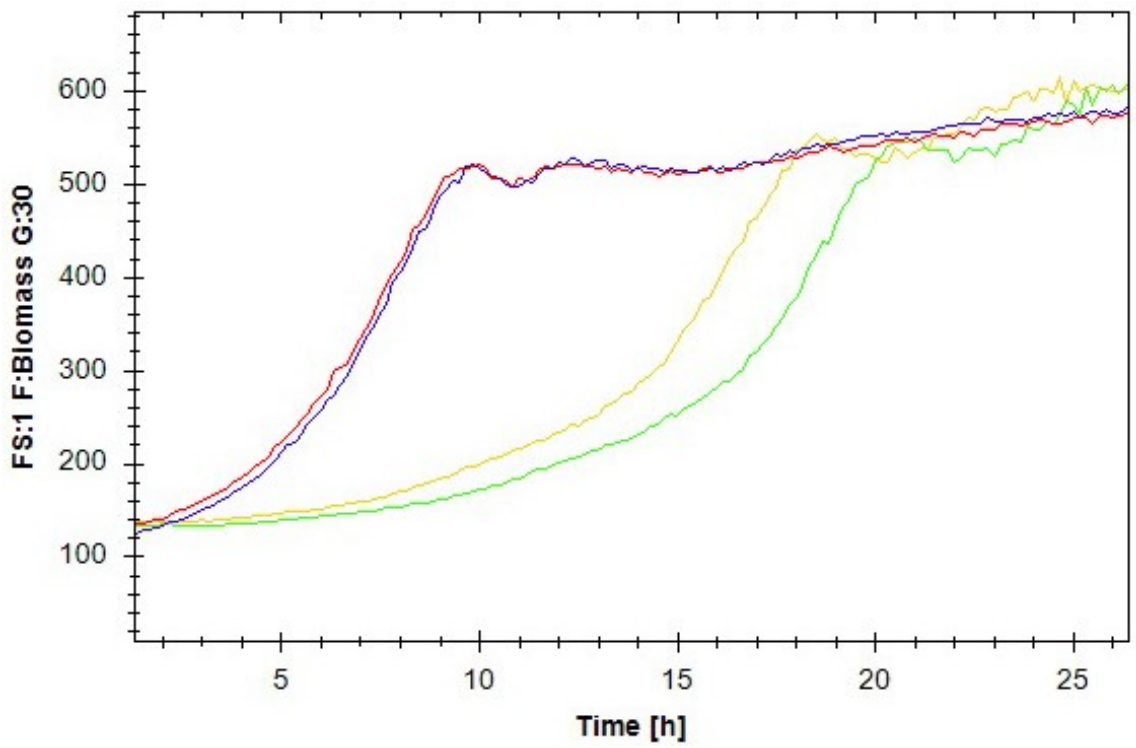

Figure 8: Biomass graph from BioLection showing wild type control (red), gaf1Δ control (blue), wild type+Torin1 15uM (green) and gaf1Δ+Torin15uM (yellow). Both strains show increased lag phase and slower exponential phase growth rate when treated with Torin1. The treated wt strain has an increased lag phase and slower exponential growth rate than the treated gaf1Δ strain suggesting gaf1Δ resistance to Torin1.

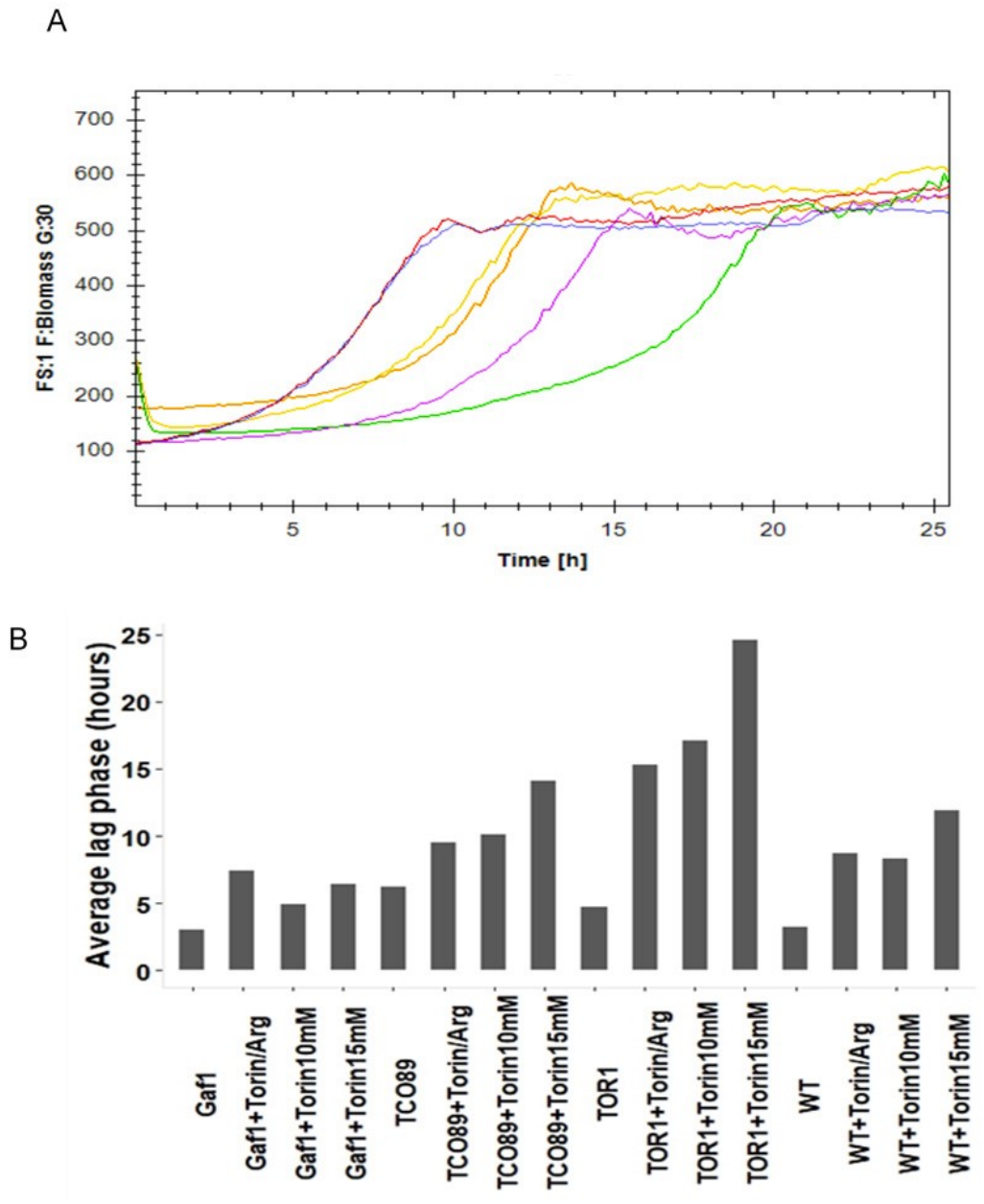

Figure 9: A) Biomass graph from BioLection showing wild type control (red), gaf1Δ control (blue), wild type + Torin1 15mM (green), gaf1Δ + Torin1 15mM (yellow), wild type + Torin15mM and arginine (purple) and gaf1Δ + Torin 15mM and arginine (orange) (B) Bar graph to show changes in lag phase length for gaf1Δ, wild type, tco89Δ and tor1Δ cells when treated with Torin 10mM, Torin 15mM and Torin 15mM + arginine. All strains except gaf1Δ showed a rescue of the increased lag phase with arginine.

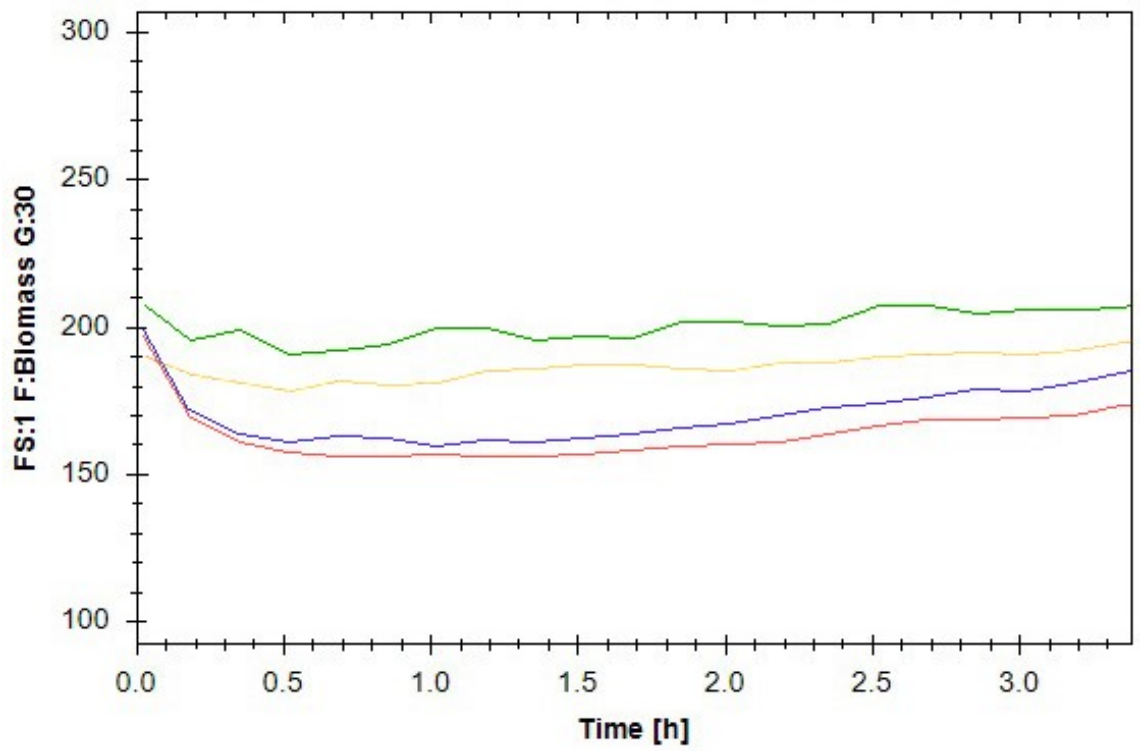

Figure 10: Biomass graph from BioLection showing arginine rescue of "Signature Torin1 Biomass Decrease" in both wild type and gaf1Δ strains: wild type and Torin1 10mM (red), gaf1Δ Torin1 10mM (blue), wild type Torin1 10mM and arginine (green) and gaf1Δ Torin1 10mM and arginine (yellow).

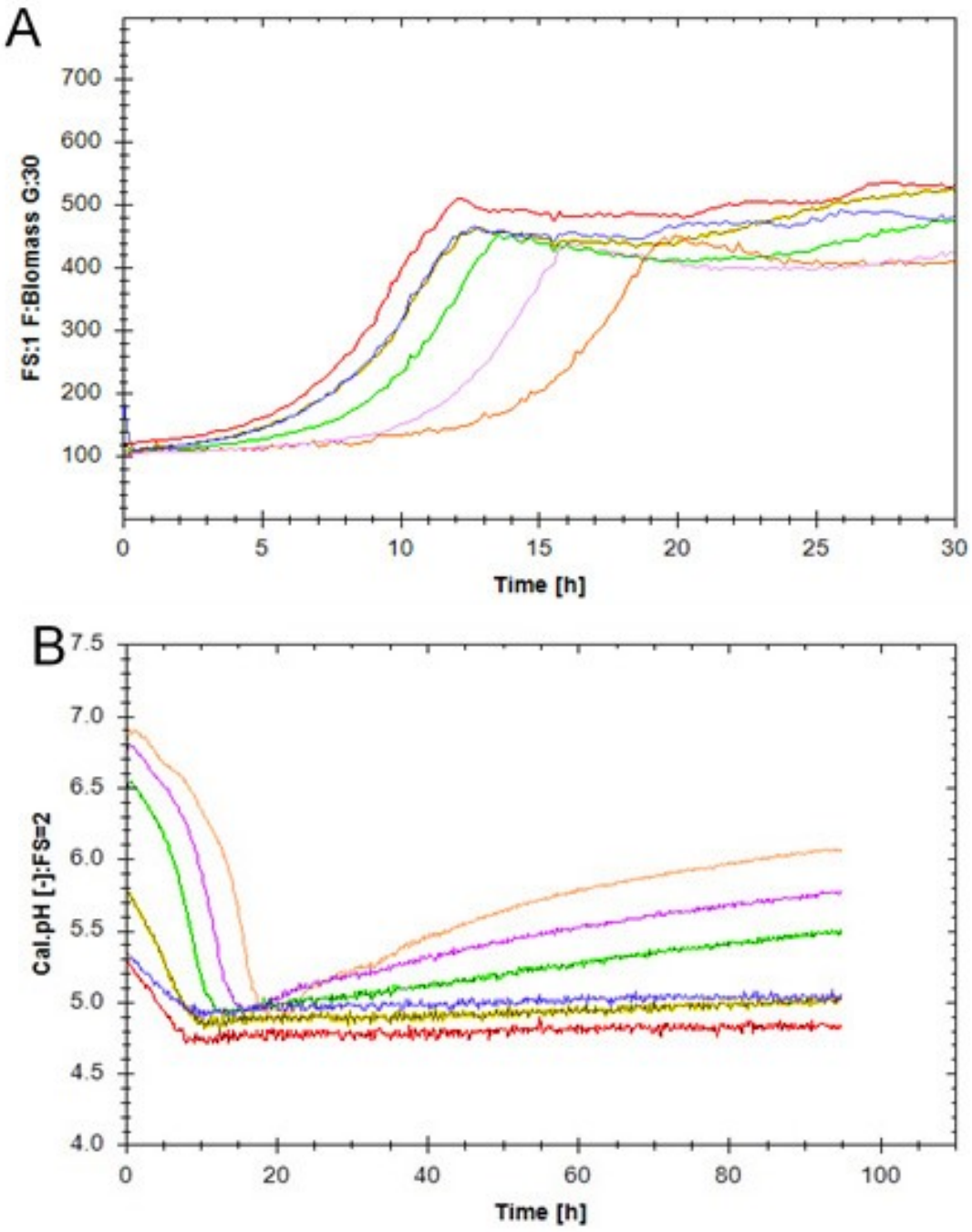

Figure 11: A)Biomass graph from BioLection showing increasing lag phase and (B) pH graph from BioLection showing increasing pH in wild type cells control (red), Torin1 2uM (blue), Torin1 2uM + arginine 4mM (yellow), Torin1 2uM + arginine 12mM (green), Torin1 2uM +arginine 16mM (purple), Torin1 2uM + arginine 20mM (orange). As the concentration of arginine increases, the pH increases and the lag phase increases.

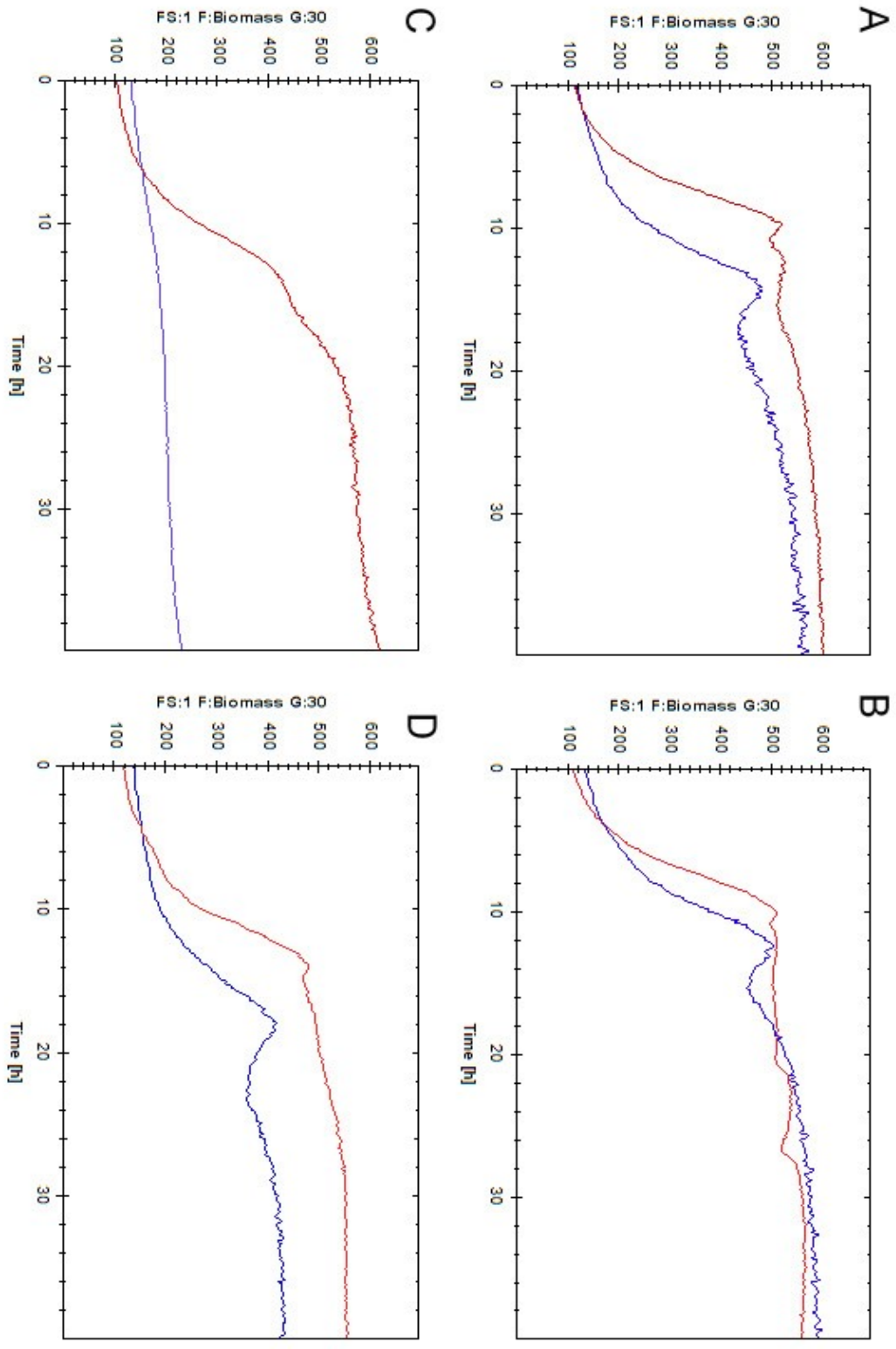

Figure 12: Biomass graph from BioLection (A) wild type, (B) gaf1Δ, (C) tor1Δ and (D) tco89Δ control (red) caffeine 10mM and rapamycin 100ng/ml (blue). gaf1Δ cells are seen to be more resistant to caffeine and rapamycin inhibition than the wild type, tor1Δ and tco89Δ strains but all strains show decreased growth with caffeine and rapamycin treatment.

Alternatively to Torin1, combined caffeine and rapamycin treatment can be used to inhibit TOR in fission yeast. 10mM caffeine and 10ng/ml rapamycin treatment of *wild type*, *gaf1*Δ, *tor1*Δ and *tco89*Δ cells inhibited growth in all cases, increasing lag phase in all cases and decreasing overall cell density in *wild type*, *tor1*Δ and *tco89*Δ. In *wild type*, *gaf1*Δ and *tco89*Δ strains a signature decrease appeared on the treated cultures immediately following exponential growth (figure 12). Nevertheless, as in the case of Torin1, *gaf1*Δ seems to be more resistant to caffeine/rapamycin combinational treatment compared to *wild type* cells. This is in accordance to previous results and genome wide screens with this drug combination(Rallis et al., 2014).

The microfermentation results give an overview of the changes in cellular growth in both *wild type* and *gaf1*Δ cells with and without TOR inhibition from a temporal perspective. TOR controls both spatial and temporal aspects of cell growth (Gonzalez and Rallis, 2017), so it is necessary to investigate if Gaf1 is involved in only temporal or also spatial aspects of TOR control.

3.3 Examining Spatial Aspects of TOR inhibition using Cell Size Microscopy

After collecting data on temporal aspects of cell growth we turned to investigating spatial aspects of cell growth. Both spatial and temporal aspects of cell growth have strong links to TOR control (Gonzalez and Rallis, 2017). We performed a time-course of Torin1 inhibition with or without arginine supplementation, coupled with microscopy and measurement of cell size changes, to record spatial downstream effects of pan-TOR inhibition.

Cell size data collected over a 60-minute period shows that *wild type* cells treated with Torin1 decrease in size from an average of 15.2 micrometres to an average of 13.8 micrometres over this time frame whereas cells treated with both Torin1 and arginine show no significant decrease in size from the original size at time zero with an average size of 15.1 micrometres after 60 minutes (figure 13 and table 6). Statistical analysis of this data using ANOVA and Turkey's multiple comparisons test in Prism (table 6) showed cells treated with Torin1 to be statistically significantly smaller than time zero to $<99^{th}$ percentile and statistically significantly smaller than those treated with Torin1 and arginine to $<95^{th}$ percentile. It showed no statistically significant difference in cell size between the time zero cells and those treated with Torin1 and arginine. Cell size was also shown to be statistically significant to $<99^{th}$ percentile between cells treated with Torin1 and measured at 15 minutes and those treated with Torin1 and measured at 60 minutes. This shows a rapid and steady decrease in cell size during this time period.

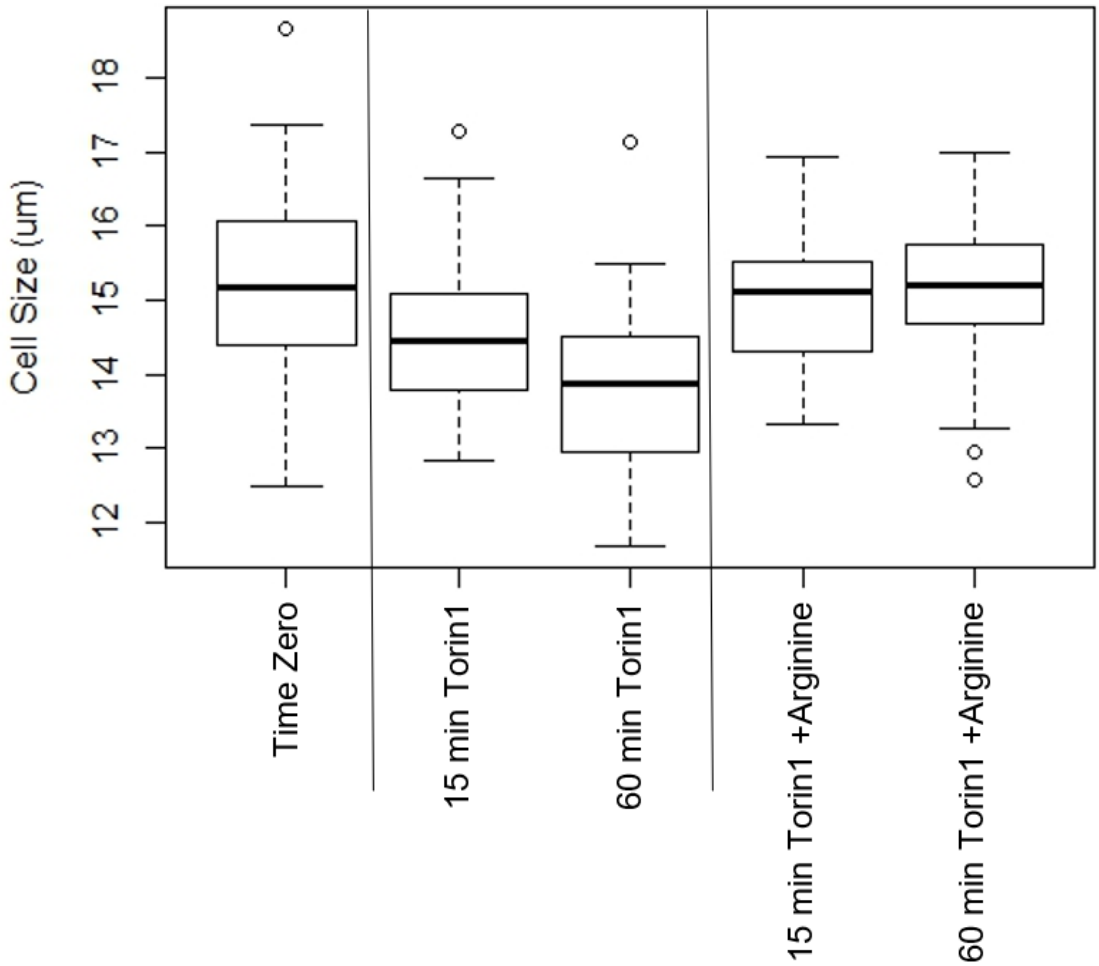

Figure 13: Box and whisker plots of wild type cell size measurements at different time points after the addition of 2μM Torin1 or 2μM Torin1 and 8mM Arginine, outliers shown as dots. Torin1 treatment without arginine reduced the cell size from time zero but Torin1 treatment with arginine did not.

Table 6: p-values for Turkey's multiple comparisons test of cell size data showing p-value for each comparison and if there is a significant difference between them. The p-values show significant differences in cell size between cells treated with only Torin1 and those treated with Torin1 and arginine at both time points.

COMPARISON	P VALUE	SIGNIFICANT?
TIME ZERO - 15MIN TORIN1	0.0227	YES
TIME ZERO - 60MIN TORIN1	<0.0001	YES
TIME ZERO - 15MIN TORIN1+ARGININE	0.9221	NO
TIME ZERO - 60MIN TORIN1+ARGININE	0.9912	NO
15MIN TORIN1 - 60MIN TORIN1	0.0013	YES
15MIN TORIN1+ARGININE - 60MIN TORIN1+ARGININE	0.9958	NO
15MIN TORIN1 - 15MIN TORIN1+ARGININE	0.1829	YES
60MIN TORIN1 - 60MIN TORIN1+ARGININE	<0.0001	YES

Subsequent analyses (not part of this MRes) of *gaf1Δ* cells with Torin1 and arginine treatments as described above indicate that arginine can 'rescue' the Torin1-induced cell size decrease in the *gaf1* mutant background as also seen in figure 10.

Given that Gaf1 is a transcription factor these temporal and spatial changes in cell growth can be further investigated in relation to Gaf1 by gene expression analysis. The growth changes seen could be due to gene expression differences between *wild type* and *gaf1*Δ cells in normal and TOR-inhibited conditions.

3.4 Gene expression analysis of wt and gaf1∆ cells using microarrays

A two-colour microarray experiment using custom made arrays (Agilent) was conducted in two biological repeats with a dye swap, to account for dye bias. Sample pools were used as reference to allow all genotypes and treatments to be directly comparable. Pooled samples were labelled with the opposite dye and used as a background comparison to all individual samples. This process was repeated with a dye swap for the duplicate samples and pool (figure 4). Duplicates were averaged and normalised before up and down regulated gene lists were produced by GenSpring. An example of the Lowess normalised data, limma and marray packages and in-house R scripts is shown in figure 14. The approach with pools and dye swaps is common in such experiments and has been successfully used in the past in numerous fission yeast studies (Rallis et al., 2013, Rallis et al., 2014).

Normalised data were inserted into the Genespring program where differentially expressed genes were extracted using standard approaches within the program. Up- and down-regulated gene lists were initially compared using an online bioinformatics tool to create Venn diagrams, shown in figure 15.

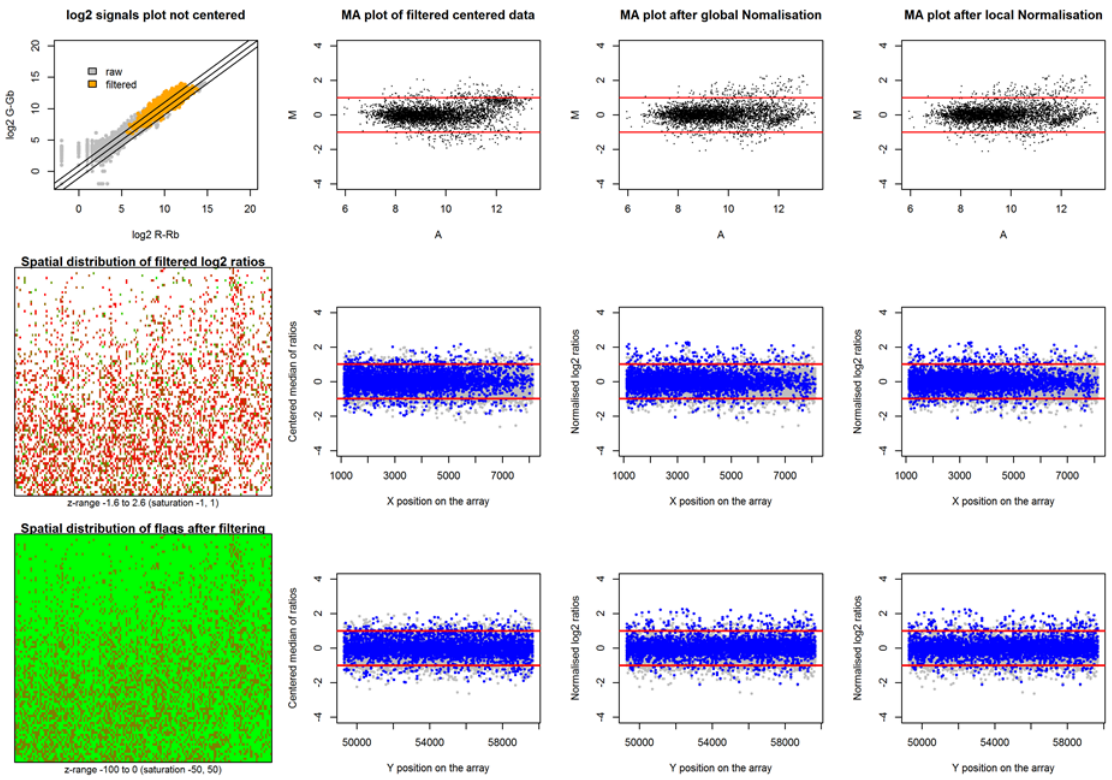

Figure 14: Microarry normalisation data for wt caffeine and rapamycin 2nd Repeat showing raw and filtered values (grey vs orange data in the top left panel) as well as cut-offs and value filtering (red horizontal lines in nine left panels). The scripts also examine local biases on the microarray that could happen due to technical reasons during hybridisations (white and green panels with red dots on the left).

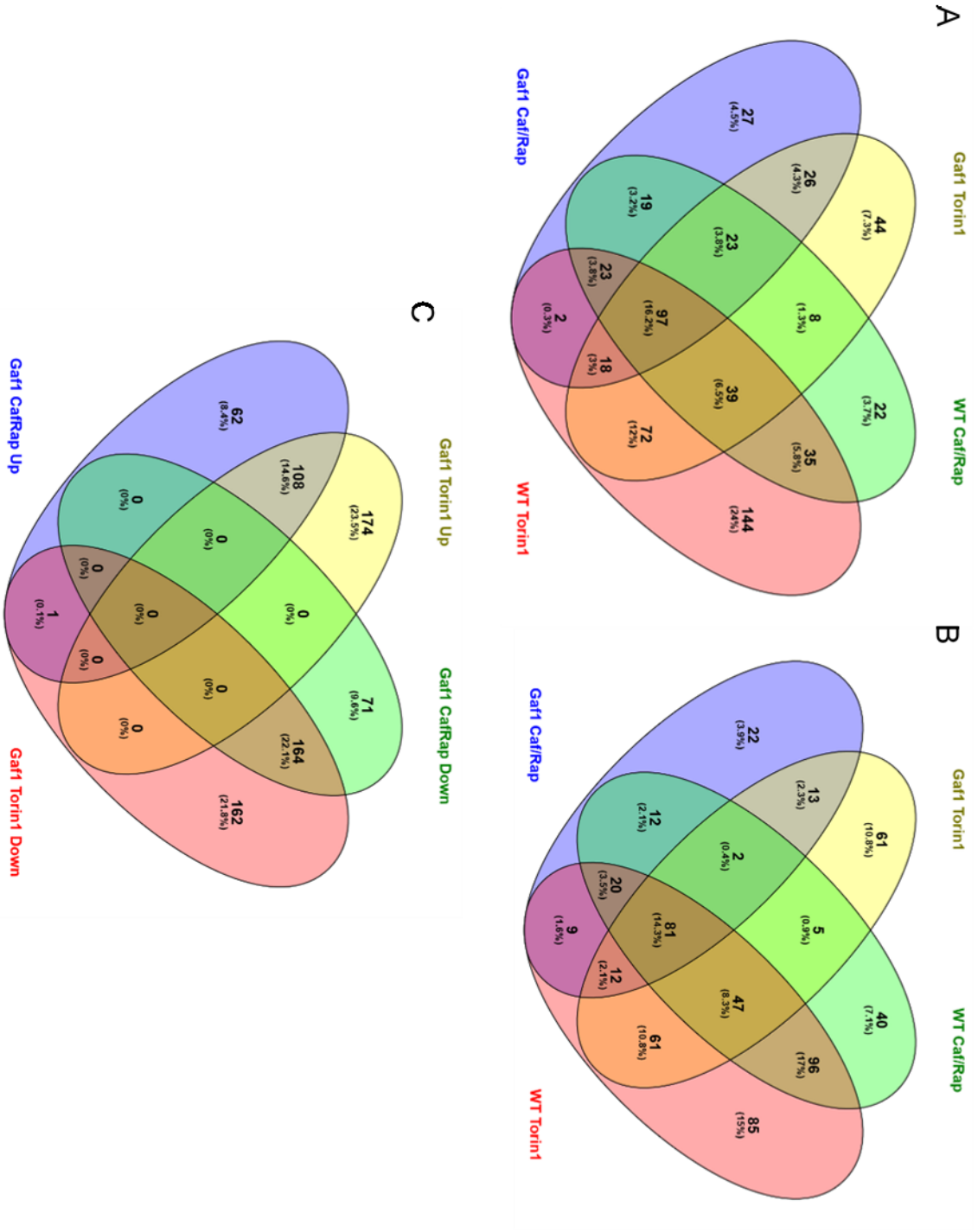

Figure 15: Venn diagrams to show overlap in (A) downregulation of genes in gaf1Δ and wild Type cells treated with caffeine and rapamycin or Torin1 (B) upregulation of genes in gaf1Δ and wild type cells treated with caffeine and rapamycin or Torin1 (C) up and downregulation of genes in gaf1Δ cells treated with caffeine and rapamycin or Torin1. Created using Gene Venn (Nagarajan, 2006).

Figure 15 A is a Venn diagram representation of downregulated genes showing 44 genes to be exclusively downregulated in Torin1 treatment of *gaf1*Δ, 100 genes less than those exclusive to the *wild type* strain treated with Torin1. The number of upregulated genes (as shown in figure 15B) were much more similar for these two categories but there were still less in the *gaf1*Δ category with 61 as opposed to 85 genes. Figure 15C shows only a single gene overlap between the up and down regulated genes in the case of both the caffeine and rapamycin and Torin1 treatments.

Gene lists produced by Venn diagram bioinformatics tools were then further analysed using a gene ontology enrichment tool, AnGeLi (BählerLab, 2015). A gene list of genes at least twofold downregulated in *wild type* cells treated with Torin1 but not at least twofold downregulated in *wild type* cells treated with caffeine and rapamycin was cross referenced with a gene list of genes at least twofold downregulated in gaf1 cells treated with Torin1 but not at least twofold downregulated in *gaf1*Δ cells treated with caffeine and rapamycin. This cross referencing produced a gene list of these genes found only in the *wild type* cells and a gene list of these genes found only in the *gaf1*Δ cells.

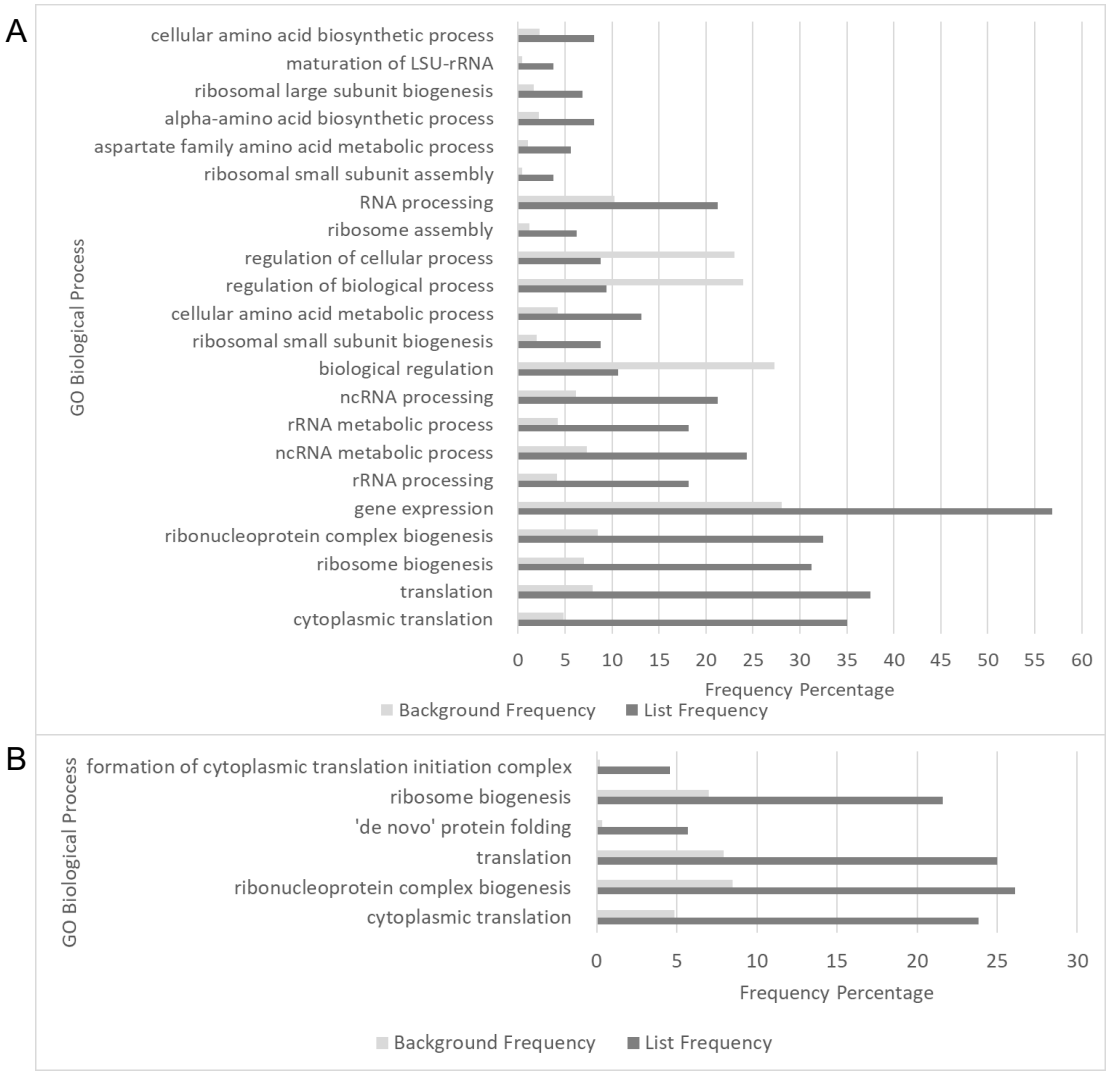

Figure 16: Bar graph to show GO enrichment percentage list frequency of >twofold change from background frequency on gene lists of (A) genes exclusively downregulated in wt treated with Torin1 and (B) genes exclusively downregulated in gaf1Δ treated with Torin1. Significantly more processes seem to be downregulated in the wt strain than the gaf1Δ strain which supports the hypothesis of gaf1Δ strain's reduced response to Torin1 treatment.

GO enrichment results which were at least a twofold change from the background frequency percentage are shown in the bar charts in figure 16. It shows an overlap in downregulation between *wild type* and *gaf1*Δ cells with regards to genes involved in translation, cytoplasmic translation, ribonucleoprotein complex biogenesis and ribosome biogenesis. Disproportionate downregulation in genes involved in formation of the cytoplasmic translation initiation complex and '*de novo*' protein folding are shown to be exclusive to *gaf1*Δ cells (figure16B), while that of those involved in the processing and metabolic processes of ribosomal RNA and non-coding RNA are shown to be exclusive to *wild type* cells (figure16A).

Gene lists were then produced in the same way of all genes either exclusive to caffeine and rapamycin treatment or found in both caffeine and rapamycin treatment and Torin1 treatment for both *gaf1*Δ and *wild type* cells. GO enrichment performed on these two lists where the list frequency showed at least a twofold change from the background frequency can be found in figure 17. Notably, rRNA and ncRNA processing and metabolic processing are seen to be strongly downregulated in both the *wild type* and *gaf1*Δ cells.

This process was then repeated to produce GO enrichment analysis for upregulated genes.

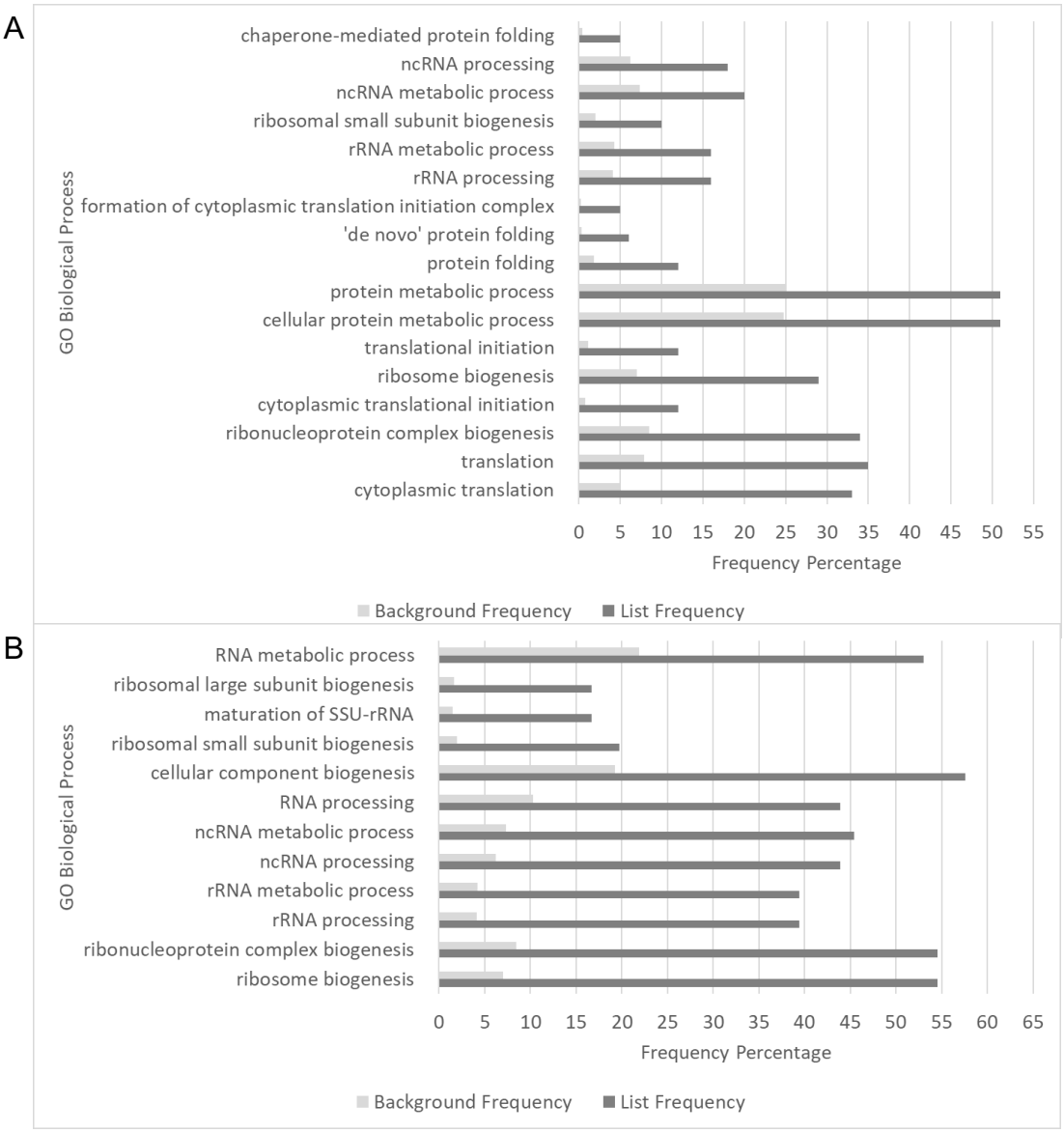

Figure 17: Bar graph to show GO enrichment percentage list frequency of >twofold change from background frequency on gene lists of (A) genes downregulated exclusively in wt treated with caf/rap and overlap downregulation in wt treated with caf/rap and wt treated with Torin1 and (B) genes downregulated exclusively in gaf1Δ treated with caf/rap and overlap downregulation in gaf1Δ treated with caf/rap and gaf1Δ treated with Torin1. There is a more similar number and range of processes seen between the wt and gaf1Δ strain downregulation in response to treatment with caffeine and rapamycin than seen in response to Torin1 treatment.

A

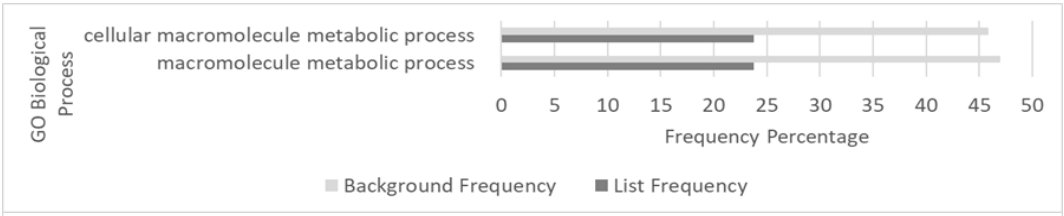
GO Biological Process
cellular macromolecule metabolic process
macromolecule metabolic process
0 5 10 15 20 25 30 35 40 45 50
Frequency Percentage
Background Frequency
List Frequency

B

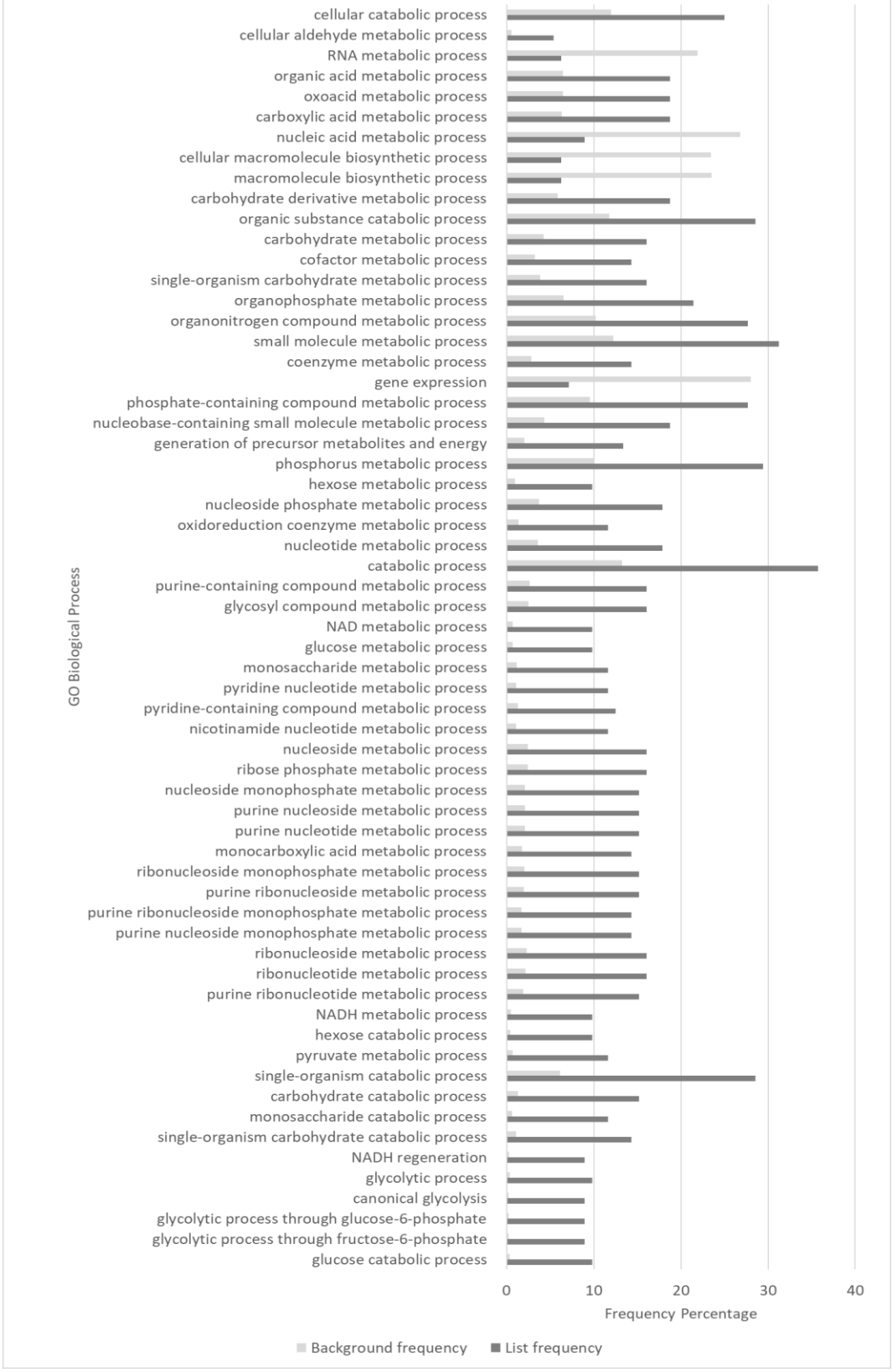
GO Biological Process
cellular catabolic process
cellular aldehyde metabolic process
RNA metabolic process
organic acid metabolic process
oxoacid metabolic process
carboxylic acid metabolic process
nucleic acid metabolic process
cellular macromolecule biosynthetic process
macromolecule biosynthetic process
carbohydrate derivative metabolic process
organic substance catabolic process
carbohydrate metabolic process
cofactor metabolic process
single-organism carbohydrate metabolic process
organophosphate metabolic process
organonitrogen compound metabolic process
small molecule metabolic process
coenzyme metabolic process
gene expression
phosphate-containing compound metabolic process
nucleobase-containing small molecule metabolic process
generation of precursor metabolites and energy
phosphorus metabolic process
hexose metabolic process
nucleoside phosphate metabolic process
oxidoreduction coenzyme metabolic process
nucleotide metabolic process
catabolic process
purine-containing compound metabolic process
glycosyl compound metabolic process
NAD metabolic process
glucose metabolic process
monosaccharide metabolic process
pyridine nucleotide metabolic process
pyridine-containing compound metabolic process
nicotinamide nucleotide metabolic process
nucleoside metabolic process
ribose phosphate metabolic process
nucleoside monophosphate metabolic process
purine nucleoside metabolic process
purine nucleotide metabolic process
monocarboxylic acid metabolic process
ribonucleoside monophosphate metabolic process
purine ribonucleoside metabolic process
purine ribonucleoside monophosphate metabolic process
purine nucleoside monophosphate metabolic process
ribonucleoside metabolic process
ribonucleotide metabolic process
purine ribonucleotide metabolic process
NADH metabolic process
hexose catabolic process
pyruvate metabolic process
single-organism catabolic process
carbohydrate catabolic process
monosaccharide catabolic process
single-organism carbohydrate catabolic process
NADH regeneration
glycolytic process
canonical glycolysis
glycolytic process through glucose-6-phosphate
glycolytic process through fructose-6-phosphate
glucose catabolic process
0 10 20 30 40
Frequency Percentage
Background frequency
List frequency

Figure 18 (previous page): Bar graph to show GO enrichment on gene lists of (A) genes exclusively upregulated in wt treated with Torin1 (all GO biological processes shown) and (B) genes exclusively upregulated in gaf1Δ treated with Torin1 (GO biological processes with percentage list frequency of >twofold change from background frequency shown). Many more processes are seen to be upregulated by the gaf1Δ strain than the wt strain during the Torin1 treatment. This supports the hypothesis of reduced downregulation in response to Torin1 treatment in the gaf1Δ strain.

Interestingly, the list of genes upregulated in *wild type* but not *gaf1*Δ cells in Torin1 treatment showed only two results from GO enrichment, while neither were quite of a twofold change from the background frequency the results have been included in figure 18A as both were of a >1.9 times decrease from the background frequency and they were the only hits found by the screen. They are similar in function with both being metabolic processing of macromolecules. Figure 18B shows the GO enrichment for the list of genes upregulated in *gaf1*Δ but not *wild type* cells during Torin1 treatment. Here a wide range of biological processes are seen to be disproportionately represented in the gene list, most notably a great number of metabolic and catabolic processes are seen to be relatively too common in the gene list.

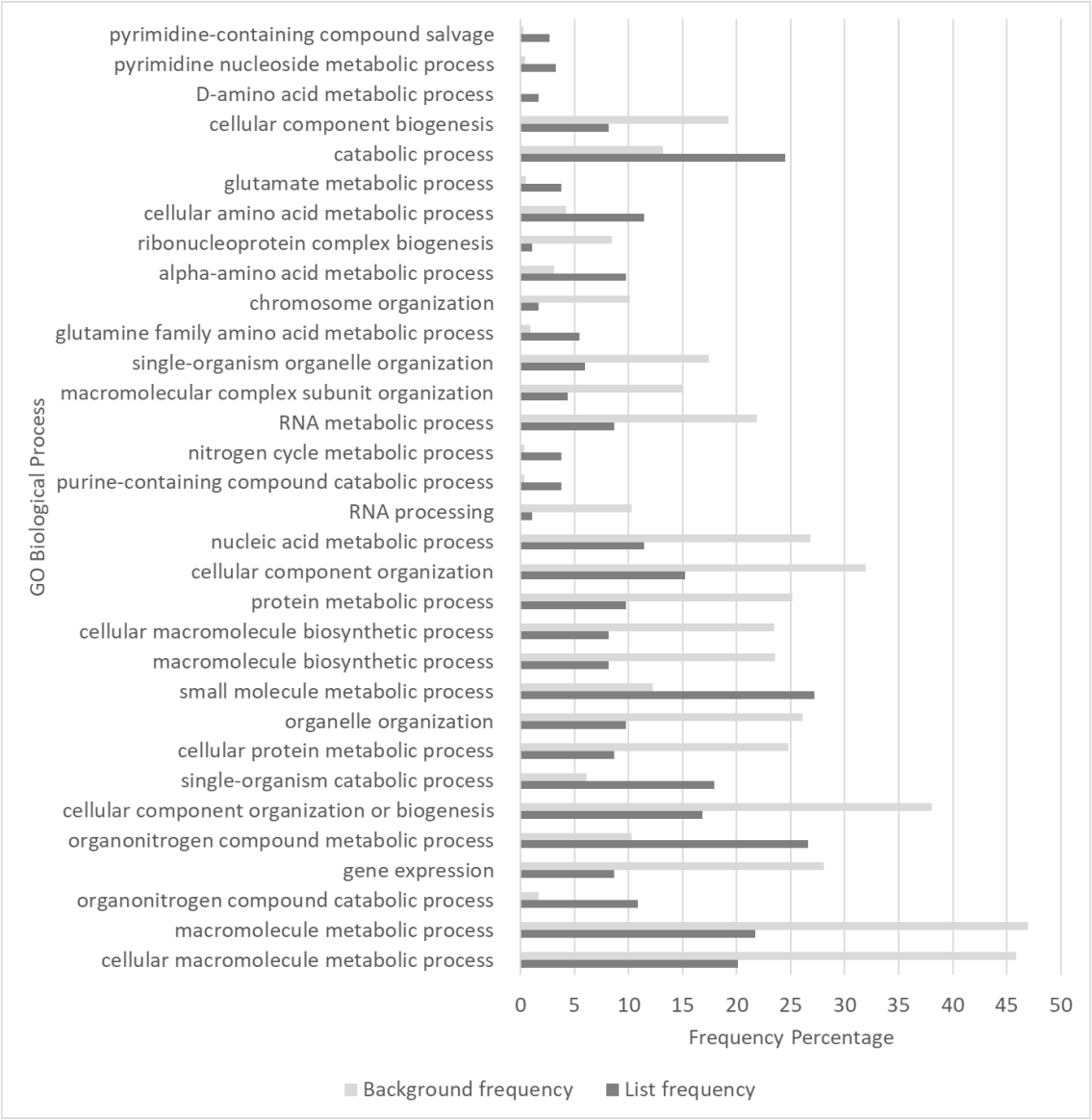

Figure 19: Bar graph to show GO enrichment percentage list frequency of >twofold change from background frequency on gene list of genes upregulated exclusively in wt treated with caf/rap and overlap downregulation in wt treated with caf/rap and wt treated with Torin1. May more processes are seen to be upregulated in the wt cells when treated with caffeine and rapamycin than when treated with Torin1.

Figure 19 shows the GO enrichment for the list of genes upregulated exclusively by *wild type* cells treated with caffeine and rapamycin and upregulated in *wild type* cells both when they are treated with caffeine and rapamycin and when they are treated with Torin1. In this dataset, organonitrogen metabolic and catabolic processes are seen to be disproportionately more common in the gene list than the background. The GO enrichment analysis of the list of genes found to be upregulated in *gaf1*Δ cells treated with caffeine and rapamycin and found to be upregulated in both *gaf1*Δ cells treated with caffeine and rapamycin or treated with Torin1 produced no GO Biological Process hits with more than a twofold change from the background frequency.

Overall, the microarray data and subsequent GO enrichment produced large amounts of data to suggest the expression changes responsible for the growth changes seen in the *gaf1*Δ phenotype during TOR inhibition. The data also suggested downstream implications of Gaf1 deletion raising the need to characterise the Gaf1 interactome.

3.5 Production of Strain for Synthetic Genetic Arrays

The initial goal of the project was to identify genes that might sensitise *gaf1Δ* to Torin1 using Synthetic Genetic Array (SGA) screening. This type of experiment would have produced a dataset of an undefined interactome of *gaf1* and a Torin1 dependent interactome highlighting genes which enhance or abolish the Torin1-resistant phenotype of *gaf1*Δ cells.

SGA analysis is a technique where a mutant of interest (query strain), in this case *gaf1*Δ*,* is mated to the entire Bioneer fission yeast deletion library (Bioneer 2010). The resulting double knockout colony sizes are used as a proxy to show if the genes have a genetic interaction and if this is positive or negative. During mating an integral step is to select for cells containing both knockout constructs, this is achieved by growth on relevant selective media. The *gaf1*Δ strain used in this study contained a kanamycin (G418) resistance gene, which is also the gene in the Bioneer deletion library. For this reason, a *gaf1*Δ strain with a different selection marker would be needed for selection of double mutants after mating.

Transformations to produce *h-gaf1*Δ*::natMX6* strain from *h-gaf1*Δ*::kanMX6* strain produced only colonies resistant to both clonNAT and G418. Fresh DNA insert was amplified by PCR and analysed by gel electrophoresis shown in figure 20A. The transformation of a *wild type* strain was attempted but did not produce any transformants. The DNA fragment for this was also synthesised by PCR and analysed by gel electrophoresis as shown in figure 20B. In both cases PCR product was cleaned up using a Qiagen PCR clean-up kit before use in the transformation protocol however this still provided no transformants. The plan for production of Gaf1 interactomes using SGAs will still be pursued within the lab but not included in this thesis.

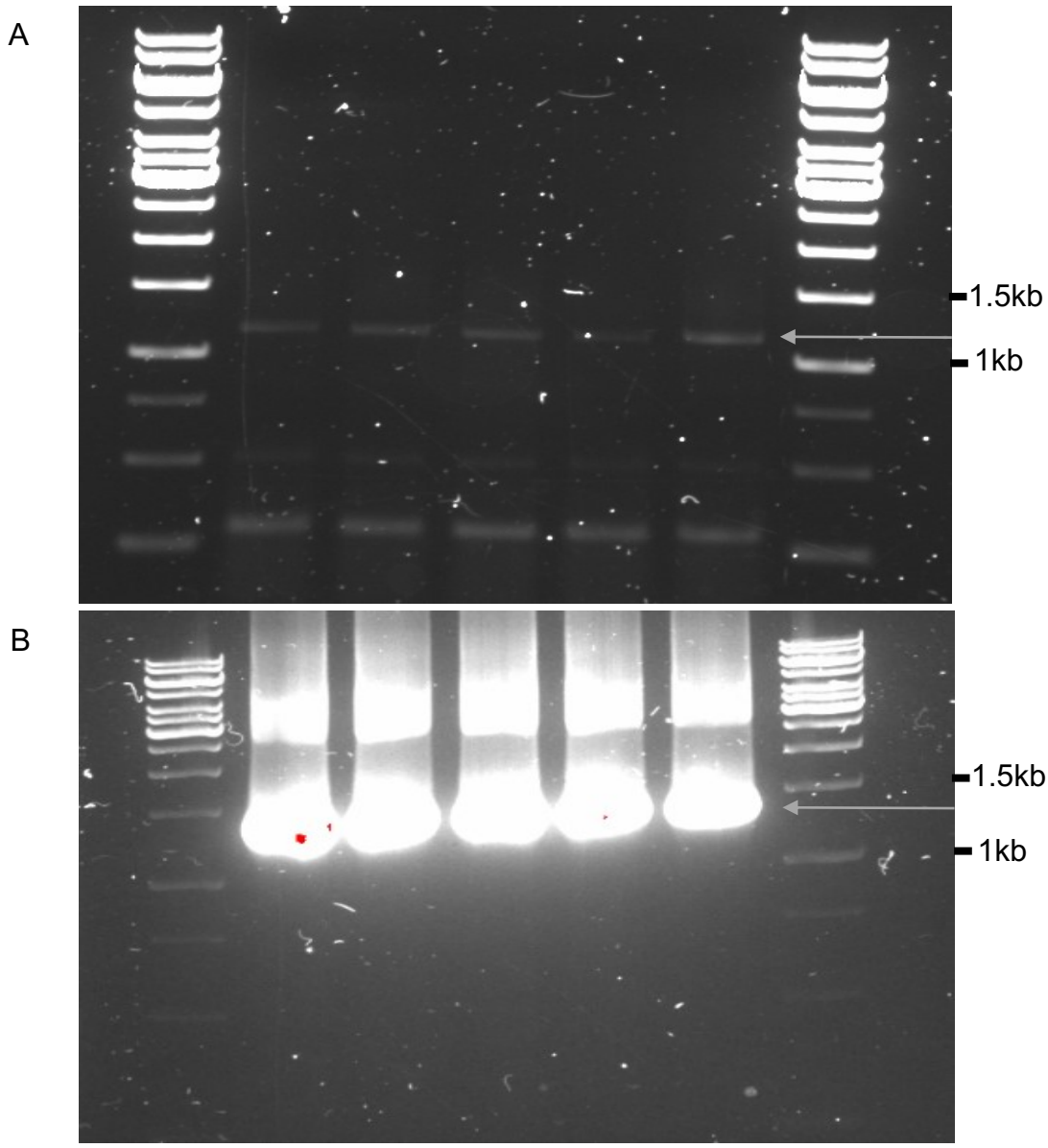

Figure 20: 1% agarose gel electrophoresis of PCR product (1.45kb) visualised using SYBR-Safe for (A) h-gaf1Δ::kanMX6 to h-gaf1Δ::natMX6 transformation (B) wild type to h-gaf1Δ::natMX6 transformation. Fragment bands are indicated between 1kb and 1.5kb ladder fragments by the grey arrow.

4 Chapter 4: Discussion

Deletion of *gaf1*, coding for a GATA transcriptional regulator results in cells that are resistant to Torin1 growth inhibition. Mutants resistant to Torin1 are related to vesicle transport (figure 6), a process also identified by a previous published screen (Lie et al., 2018). However, to date, *gaf1* has not been involved with this biological process. Nevertheless, the Gaf1 orthologue in budding yeast, Gat1, has been shown to be to be strongly connected with vacuole and vesicle transport (Fayyadkazan et al., 2014, Kingsbury and Cardenas, 2016). To better understand the underlying mechanism of the resistance of *gaf1*Δ to Torin1, the mutants found resistant in our screen were cross-referenced with predicted protein interactions with *gaf1* (figure 7). Two genes were identified as both resistant to Torin1 inhibition and as predicted to physically interact with Gaf1 protein (table 5). The gene with the strongest confidence in prediction, *php5*, is involved in regulation of transcription via RNA polymerase II. This function is closely related to a *gaf1* function: RNA polymerase II proximal promoter sequence-specific DNA binding (Pombase). The other gene identified, *shd1* (cytoskeletal protein binding protein Sla1 family), codes for a protein involved in vesicle-mediated transport and this could present a potential way that *gaf1*Δ resistance is also vesical transport mediated. Interestingly *shd1* has been shown to be long lived in a previous caffeine and rapamycin screen (Rallis et al., 2014) implicating it in TORC1 signalling. Intracellular trafficking and endocytosis have been found to contribute to necrotic neurodegeneration (Troulinaki and Tavernarakis, 2012) and therefore *shd1*-mediated lifespan extension would be a gene of interest for future ageing studies. Both *php5* and *shd1* would be genes of interest in a future synthetic genetic array experiment to investigate their interaction with *gaf1*.

The use of a library screen is very useful as a tool to quickly identify, in genomic scale, genes which are particularly resistant to or sensitised by certain nutritional or pharmacological factors, such as Torin1; however the screen is very much an initial experiment and requires follow-up experiments. Some results of the screen can be considered unreasonable and were excluded from the final result list. For example, this screen identified genes which had colony size ratios of 212 and 232. These ratios are not necessarily inaccurate however it is advisable to be cautious of such extreme results as they are likely to not be

reproducible. As a next step it is important to establish a gene of interest's Torin1 resistance by other methods to verify the library screen results. This can be done in several ways such as using stress spot plate experiments, chronological lifespan assays or microfermentation. As well as this, screens can be compared to previous published library screens to help establish their reliability. The results of this screen showed a strong similarity with the results from the published screen in not only identified gene hits but also GO metabolic processes (Lie et al., 2018).

Spotting serial dilutions of mutant cultures on plates are a similar experiment to the library screen and can produce only limited data as, due to their qualitative nature, they are unable to provide insight into the growth curve of the cells; therefore, they are more appropriate for use as a quick validation method than an actual experimental measurement for which a quantitative method is preferable. For this study microfermentation, which provides quantitative growth aspects was preferable to lifespan assays as the data is produced much more quickly and therefore many more conditions could be studied in a relatively limited time frame. In addition, the effect of Torin1 on the chronological lifespan of fission yeast is an integrated part of another study within the lab and is not the focus of this thesis.

Figure 8 shows that *gaf1*Δ cells are resistant to Torin1 inhibition compared to *wild type* cells with regards to lag phase. This confirms the resistance shown in the library screen and clearly shows that the difference in growth kinetics can be potentially explained by the decreased lag phase. Figure 8 also highlighted a signature decrease in biomass in response to Torin1 in both *gaf1*Δ and *wild type* cultures. To rescue the effects of Torin1 inhibition, arginine, a potent TOR stimulator (Yuan et al., 2015), was added to the cultures. This notably rescued the lag phase in *wild type* but not *gaf1*Δ cells; however, it rescued the signature decrease in biomass in both (figure 9). The same microfermentation experiment included *tor1*Δ and *tco89*Δ (a functional deletion mutant of a fission yeast TORC1 core component) and both cultures here also showed lag phase rescue with the addition of arginine. This suggests that potentially the arginine lag phase rescue effect is a Gaf1-dependent process related to Gaf1's role in stimulating amino acid uptake in response to TOR inhibition via *isp7 (Laor et al., 2014)*.

To find the optimum arginine concentration for lag phase rescue in *wild type* a microfermentation experiment was set up to include a range of arginine concentrations. Figure 11A shows that increasing levels of arginine results in increasing lag phases rather than the rescue that had previously been seen. To identify the cause of this, pH was also measured in an identical experimental setup and the rapidly increasing pH shown in figure 11B correlates exactly with the biomass with the pH levelling and the biomass effect ending at ~10-16 hours respectively. This led to the conclusion that while arginine can rescue Torin1-induced lag phase extension, when increasing arginine concentration increases the pH of the culture too much this effect is overridden by the effect of more alkaline conditions. This means that a more effective arginine treatment could be created by pH correcting media plus arginine in future experiments.

Interestingly, the rescue of the signature decrease in biomass appears independent of the pH changes and is unlikely to have been caused by them since Torin1 treatment itself increases pH from the control but less so than low concentrations of arginine. Figure 10 shows that the Torin1-dependent decrease in biomass seen in both *wt* and *gaf1*Δ can be rescued by addition of arginine to the culture. This decrease in biomass was hypothesised to be caused by a reduction in cell size, supported by the data in figure 13. Here it is shown that, at both time points, the addition of Torin1 significantly reduced cell size from time zero however the addition of Torin1 and arginine did not, clearly showing that arginine does rescue a cell size reduction in Torin1 treatment. Potentially this reduction in cell size could be due to temporal aspects of the cell cycle alteration causing the cells to divide earlier or spatial aspects of cell growth such as metabolic dependent cell size in response to treatment by Torin1 (Gonzalez and Rallis, 2017, Rallis et al., 2013). *gaf1*Δ cells show the same signature as the *wild type* cells, so it can be theorised that this is also due to a reduction in cell size. The data suggests that lag phase rescue in response to arginine treatment is Gaf1 and pH dependent whereas the cell size rescue is Gaf1 and pH independent.

Temporal aspects of cell growth have long been associated with TORC1 and spatial aspects of cell growth with TORC2, however recent research suggests a crossover of functions (Gonzalez and Rallis, 2017). TORC1 inhibition should lead to Gaf1 dephosphorylation and consequent migration into the nucleus

(Laor et al., 2015). In *gaf1*Δ cells the loss of downstream Gaf1 functions are believed to be the cause of Torin1 resistance so it is an interesting point for further research that the deletion of Gaf1 and its downstream targets have no effect on the signature biomass decrease potentially caused by cell size reduction but does affect temporal aspects such as cellular lifespan and lag phase.

In this study, the biomass decrease is a feature seen in Torin1 TOR inhibition but not caffeine and rapamycin TOR inhibition. It is known that caffeine and rapamycin inhibition of TORC1 causes cell size reduction by advancing mitotic onset (Gonzalez and Rallis, 2017, Rallis et al., 2013). With this in mind, while previous literature shows that cell size can be TORC1 dependent (Rallis et al., 2013), the biomass decrease was not seen in the caffeine and rapamycin results through microfermentation analysis, suggesting that further study surrounding the mechanism would be needed to fully determine the involvement of TORC1/TORC2 in this phenomenon. Figure 12 shows an unexplained decrease in biomass in caffeine and rapamycin treatment at ~20 hours not present on the controls in *gaf1*Δ, *wt* and *tco89*Δ but not *tor1*Δ, the functional knockout of TORC2. There is a potential for further study of cell size at this point as it is known that prolonged treatment with rapamycin causes TORC2 inhibition. Correlating cell size microscopy data could potentially suggest that this response could be TORC2 mediated as well as the already known TORC1 involvement (Rallis et al., 2013). The theory that the Torin1 dependent decrease in cell size could be TORC2 dependent would explain how it could be Gaf1 independent as Gaf1 is directly dephosphorylated by TORC1 inhibition but it's involvement with TORC2 is currently undefined and may be less direct.

Gene expression analysis was performed using a custom microarray platform. This technique was chosen over alternatives because microarrays were already an established pipeline within the lab and the technique was less expensive than other options, such as RNA-Seq. Microarray analysis is an established and reliable method of expression analysis, however there are limitations; microarrays are not an open platform such as RNA-Seq meaning that the technique is restricted by the pre-chosen number of gene probes included within the array. Microarrays are also affected by cross or non-specific hybridisation background noise. During the lowess normalisation and analysis

of microarrays, a statistical assumption is made that most genes show no change. This means that some small expression changes may not be detected if they are hidden by this assumption.

Microarray analysis was used to study the expression differences between *wild type* and *gaf1*Δ fission yeast treated with Torin1 as well as with a combination of caffeine and rapamycin. These results are likely to be valid due to the dye swap used to eliminate dye bias and the fact that untreated and fast growing *gaf1*Δ and *wild type* cells showed no difference in expression (data not shown). This indicates that expression changes seen are likely to be due solely to the cell's response to treatment.

Microarray data was processed to produce gene lists of up and downregulated genes for each parameter and these lists were initially compared using Venn diagrams shown in figure 15. Here there are 100 more genes exclusively downregulated in *wild type* cells in response to Torin1 treatment than in *gaf1*Δ cells in response to Torin1 treatment (figure 15A) with more similar results seen for upregulation (figure 15B). Figure 15C showed virtually no overlap between upregulated and downregulated genes in the *gaf1*Δ samples further evidencing the validity of the microarray results. This initial Venn diagram analysis demonstrated the heavy involvement of Gaf1 in regulating genes downstream of TOR and the need to further analyse these gene lists to identify Gaf1-dependent cellular functions. To do this gene ontology enrichment analysis was performed using the AnGeLi online bioinformatics tool.

Downregulated genes seen only in *wild type* but not *gaf1*Δ cells in response to Torin1 inhibition (figure 15A and 16A) are shown to be disproportionately involved in a wide range of biological processes. Some downregulation is likely to be Gaf1 dependent. Genes involved in translation, cytoplasmic translation, ribonucleoprotein complex biogenesis and ribosome biogenesis are shown to be downregulated in both *wild type* and *gaf1*Δ cells and so are likely not to be *gaf1*-dependent processes. Genes involved in rRNA and ncRNA processing and metabolic process are notably downregulated exclusively in the *wild type* cells suggesting *gaf1*Δ dependence in these processes. Cellular amino acid biosynthesis and metabolic process genes are also notably downregulated disproportionately in *wild type* cells which is interesting given Gaf1's known involvement in increased amino acid uptake (Laor et al., 2014). Potentially this

could be to accumulate amino acids within the cell without metabolising them in response to TOR inhibition which is naturally caused by lack of nutrient availability.

Figure 16B highlights that genes involved in the formation of the cytoplasmic initiation complex and *de novo* protein folding are disproportionately present in the *gaf1*Δ Torin1 downregulated genes list. This suggests that these two processes are either directly or indirectly upregulated by Gaf1 or that their downregulation is prevented by Gaf1 in *wild type* cells. This data is consistent with the current knowledge that Gaf1 stimulates amino acid uptake during TOR inhibition (Laor et al., 2014) thought to be part of a process which allows Gaf1 to immediately compensate for TOR inhibition in a cell. In this way, Gaf1 could also be responsible for stimulating other cell processes necessary for survival such as the translation and protein synthesis involvement seen here. Genes involved in the regulation of cellular processes and regulation of biological processes are seen to be disproportionately absent from the *wild type* downregulation shown in figure 16A, supporting this hypothesis that Torin1 treatment leads to Gaf1 dependent stimulation of cellular processes to compensate for TOR inhibition.

The distinct reduction in downregulated genes in response to Torin1 inhibition in *gaf1*Δ cells, compared to *wild type* cells could account for *gaf1*Δ resistance to Torin1 in terms of growth. Gaf1-dependent downregulation of rRNA and ncRNA processing and metabolic process included ten genes directly involved with tRNAs, supporting current ChIP-seq data that Gaf1 can directly regulate tRNA expression, following TOR inhibition (Rodriguez-Lopez, Gonzalez *et al.,* unpublished). The data so far suggest that Gaf1 is directly implicated in tRNA regulation following stresses and thus affecting cellular recovery and growth. Figure 17 further develops this picture, showing rRNA and ncRNA processing and metabolic processes are seen to be downregulated in both *wild type* and *gaf1*Δ cells. Further experiments including northern analyses of tRNAs in Torin1-treated and untreated *wt* and *gaf1*Δ backgrounds have shown that Gaf1 regulates tRNA expression. Additional tests are necessary to develop and evidence which Gaf1 mediated effects are TORC1 and TORC2 dependent as this study has so far only highlighted the possibility of a more complicated interplay between Gaf1 and the TOR complexes without defining it.

The GO enrichment in figure 18 shows that in *wild type* cells, treated with Torin1, upregulation of macromolecule metabolism and catabolism was disproportionately absent, while upregulation of metabolism and catabolism was disproportionately present in *gaf1*Δ cells, treated with Torin1. This supports the idea that Gaf1 is implicated in organonitrogen metabolism, namely that of amino acids and nucleotides. Inhibition of TOR should lead to a reduction in metabolic processes (Laplante and Sabatini, 2012) as seen in the *wild type* cells treated with Torin1 however the upregulation of these processes seen in the *gaf1*Δ cells treated with Torin1 suggests that Gaf1 is integral to the suppression of some metabolic processes during TOR inhibition.

Figure 19 shows the GO enrichment for the list of genes upregulated exclusively in *wild type* cells treated with caffeine and rapamycin and those upregulated both when *wild type* cells are treated with caffeine and rapamycin or Torin1. Here we see upregulation of organonitrogen metabolic processes but a lack of upregulation for several other metabolic processes. Interestingly the list for upregulated genes in *gaf1*Δ cells when treated with caffeine and rapamycin and upregulated when treated with either caffeine/rapamycin or Torin1 produced no GO enrichment hits so it cannot be used as a comparison. However, in the Torin1 inhibition of *gaf1*Δ cells we see that upregulation of organonitrogen processes but not of other metabolic and catabolic processes suggesting there may be little to no change between the *wild type* and *gaf1*Δ in this respect. It is known that GATA transcription factors in budding yeast, including the Gaf1 orthologue Gat1 are involved in nitrogen catabolite repression sensitive gene expression control (Cooper, 2002) and recent ChIP-seq data (Rallis, personal communication) suggests Gaf1 regulates organonitrogen compound genes and potentially plays a role in nitrogen catabolite repression, highlighting the need for further investigation in this area as the GO enrichment analysis in this study appears to contradict present data.

Following on from these results that suggest a plethora of Gaf1 transcriptional controls and downstream effects it was deemed useful to create a picture of the Gaf1 genetic interactome, this was planned using synthetic genetic array (SGA) analysis. Here the *gaf1*Δ query strain would have been mated with the fission yeast deletion library (Bioneer Version 5, containing ~3500 mutants) producing data evidencing *gaf1's* involvement in cellular processes and pathways. This

required a *gaf1*Δ strain with a selective marker different from the library knockouts to allow for double mutant selection after mating.

To construct this strain a transformation using a *natMX6* cassette was attempted multiple times with 12 method adaptations, however, even after fresh DNA was produced by PCR (figure 20A), no successful colonies were obtained. On two occasions a cell line resistant to both G418 and clonNAT was generated suggesting that the fragment had inserted itself into a different locus. For this reason, the cassette was amplified from the plasmid again using new primers for generating an independent *gaf1*Δ knockout directly from *wild type* cells (figure 20B) which has larger homology regions. Using this approach we generated much more DNA for transformations, however no transformants were obtained. Due to time constraints on the MRes project it was impossible to continue attempts to produce the strain necessary and therefore also impossible to carry out the planned SGAs. Given more time adaptations to the methodology for the *wild type* knockout would have been made until the transformation was successful. Alternatively, a CRISPR/Cas9 approach could have been used to create the strain as it would likely have been successful however time constraints did not allow this approach.

In conclusion, the study has evidenced Gaf1 involvement with TORC1 in line with current knowledge while highlighting potential for Gaf1 involvement with TORC2. The *gaf1*Δ resistance to Torin1 has been shown to be potentially mediated by control of rRNA and ncRNAs including tRNAs, consistent with current emerging data about Gaf1-dependent gene regulation. ChIP-seq experiments performed by the lab but not part of this thesis have confirmed fission yeast Gaf1 binding to all tRNAs and ncRNAs. Genes of interest in the mechanism of *gaf1*Δ resistance to TOR inhibition by Torin1 have been identified by PInt prediction and a Torin1 library screen presenting suggestions for further study. One of these genes also presents a possible candidate for *gaf1*Δ's Torin1 resistance to be connected to vesicle transport which has been highlighted by the library screen as a major cause of Torin1 resistance.

5 References

ABRAHAM, R. T. 1998. Mammalian target of rapamycin: immunosuppressive drugs uncover a novel pathway of cytokine receptor signaling. *Curr Opin Immunol,* 10**,** 330-6.

ARONOVA, S., WEDAMAN, K., ANDERSON, S., YATES, J., 3RD & POWERS, T. 2007. Probing the membrane environment of the TOR kinases reveals functional interactions between TORC1, actin, and membrane trafficking in Saccharomyces cerevisiae. *Mol Biol Cell,* 18**,** 2779-94.

BÄHLERLAB. *Resources* [Online]. Available: http://www.bahlerlab.info/resources/ [Accessed 2018].

BÄHLERLAB. 2015. *AnGeLi* [Online]. Available: AnGeLihttp://bahlerweb.cs.ucl.ac.uk/cgi-bin/GLA/GLA_input [Accessed].

BEAUCHAMP, E. M. & PLATANIAS, L. C. 2013. The evolution of the TOR pathway and its role in cancer. *Oncogene,* 32**,** 3923-32.

BHOLA, N. E., JANSEN, V. M., KOCH, J. P., LI, H., FORMISANO, L., WILLIAMS, J. A., GRANDIS, J. R. & ARTEAGA, C. L. 2016. Treatment of Triple-Negative Breast Cancer with TORC1/2 Inhibitors Sustains a Drug-Resistant and Notch-Dependent Cancer Stem Cell Population. *Cancer Res,* 76**,** 440-52.

BIONEER. 2010. *S. pombe Deletion Mutant Library from Bioneer* [Online]. Available: https://us.bioneer.com/products/spombe/spombeoverview.aspx [Accessed 29/10/2018 2018].

BLENIS, J. 2017. TOR, the Gateway to Cellular Metabolism, Cell Growth, and Disease. *Cell,* 171**,** 10-13.

BROWN, E. J., ALBERS, M. W., SHIN, T. B., ICHIKAWA, K., KEITH, C. T., LANE, W. S. & SCHREIBER, S. L. 1994. A mammalian protein targeted by G1-arresting rapamycin-receptor complex. *Nature,* 369**,** 756-8.

COOPER, T. G. 2002. Transmitting the signal of excess nitrogen in Saccharomyces cerevisiae from the Tor proteins to the GATA factors: connecting the dots. *FEMS microbiology reviews,* 26**,** 223-238.

DAZERT, E. & HALL, M. N. 2011. mTOR signaling in disease. *Curr Opin Cell Biol,* 23**,** 744-55.

EUROFINSGENOMICS. 2019. *DNA & RNA oligonucleotides* [Online]. Available: https://www.eurofinsgenomics.eu/en/dna-rna-oligonucleotides.aspx [Accessed].

FAYYADKAZAN, M., TATE, J. J., VIERENDEELS, F., COOPER, T. G., DUBOIS, E. & GEORIS, I. 2014. Components of Golgi-to-vacuole trafficking are required for nitrogen- and TORC1-responsive regulation of the yeast GATA factors. *MicrobiologyOpen,* 3**,** 271-287.

GONZALEZ, S. & RALLIS, C. 2017. The TOR Signaling Pathway in Spatial and Temporal Control of Cell Size and Growth. *Front Cell Dev Biol,* 5**,** 61.

GRAPHPADSOFTWARE. 2018. *Prism* [Online]. Available: https://www.graphpad.com/scientific-software/prism [Accessed].

HEITMAN, J., MOVVA, N. R. & HALL, M. N. 1991a. Targets for cell cycle arrest by the immunosuppressant rapamycin in yeast. *Science,* 253**,** 905-9.

HEITMAN, J., MOVVA, N. R., HIESTAND, P. C. & HALL, M. N. 1991b. FK 506-binding protein proline rotamase is a target for the immunosuppressive agent FK 506 in Saccharomyces cerevisiae. *Proc Natl Acad Sci U S A,* 88**,** 1948-52.

HELLIWELL, S. B., WAGNER, P., KUNZ, J., DEUTER-REINHARD, M., HENRIQUEZ, R. & HALL, M. N. 1994. TOR1 and TOR2 are structurally and functionally similar but not identical phosphatidylinositol kinase homologues in yeast. *Mol Biol Cell,* 5**,** 105-18.

JOHNSON, S. C. & KAEBERLEIN, M. 2016. Rapamycin in aging and disease: maximizing efficacy while minimizing side effects. *Oncotarget,* 7**,** 44876-8.

JOHNSON, S. C., RABINOVITCH, P. S. & KAEBERLEIN, M. 2013. mTOR is a key modulator of ageing and age-related disease. *Nature,* 493**,** 338-45.

KIM, L., HOE, K. L., YU, Y. M., YEON, J. H. & MAENG, P. J. 2012. The fission yeast GATA factor, Gaf1, modulates sexual development via direct down-regulation of ste11+ expression in response to nitrogen starvation. *PLoS One,* 7**,** e42409.

KINGSBURY, J. M. & CARDENAS, M. E. 2016. Vesicular Trafficking Systems Impact TORC1-Controlled Transcriptional Programs in Saccharomyces cerevisiae. *G3: Genes|Genomes|Genetics,* 6**,** 641-652.

KSCHISCHO, M. K. A. G. H. A. H. L.-F. A. J. L. A. M. 2010. grofit: Fitting Biological Growth Curves with R. *Journal of Statistical Software, Articles,* 33**,** 1-21.

KUNZ, J., HENRIQUEZ, R., SCHNEIDER, U., DEUTER-REINHARD, M., MOVVA, N. R. & HALL, M. N. 1993. Target of rapamycin in yeast, TOR2, is an essential phosphatidylinositol kinase homolog required for G1 progression. *Cell,* 73**,** 585-96.

LAOR, D., COHEN, A., KUPIEC, M. & WEISMAN, R. 2015. TORC1 Regulates Developmental Responses to Nitrogen Stress via Regulation of the GATA Transcription Factor Gaf1. *MBio,* 6**,** e00959.

LAOR, D., COHEN, A., PASMANIK-CHOR, M., ORON-KARNI, V., KUPIEC, M. & WEISMAN, R. 2014. Isp7 is a novel regulator of amino acid uptake in the TOR signaling pathway. *Mol Cell Biol,* 34**,** 794-806.

LAPLANTE, M. & SABATINI, D. M. 2009. mTOR signaling at a glance. *J Cell Sci,* 122**,** 3589-94.

LAPLANTE, M. & SABATINI, D. M. 2012. mTOR signaling in growth control and disease. *Cell,* 149**,** 274-293.

LEONTIEVA, O. V. & BLAGOSKLONNY, M. V. 2016. Gerosuppression by pan-mTOR inhibitors. *Aging (Albany NY),* 8**,** 3535-49.

LEONTIEVA, O. V., DEMIDENKO, Z. N. & BLAGOSKLONNY, M. V. 2015. Dual mTORC1/C2 inhibitors suppress cellular geroconversion (a senescence program). *Oncotarget,* 6**,** 23238-48.

LIE, S., BANKS, P., LAWLESS, C., LYDALL, D. & PETERSEN, J. 2018. The contribution of non-essential Schizosaccharomyces pombe genes to fitness in response to altered nutrient supply and target of rapamycin activity. *Open Biol,* 8.

LIU, Q., XU, C., KIRUBAKARAN, S., ZHANG, X., HUR, W., LIU, Y., KWIATKOWSKI, N. P., WANG, J., WESTOVER, K. D., GAO, P., ERCAN, D., NIEPEL, M., THOREEN, C. C., KANG, S. A., PATRICELLI, M. P., WANG, Y., TUPPER, T., ALTABEF, A., KAWAMURA, H., HELD, K. D., CHOU, D. M., ELLEDGE, S. J., JANNE, P. A., WONG, K.-K., SABATINI, D. M. & GRAY, N. S. 2013. Characterization of Torin2, an ATP-competitive inhibitor of mTOR, ATM and ATR. *Cancer research,* 73**,** 2574-2586.

LOEWITH, R. & HALL, M. N. 2011. Target of rapamycin (TOR) in nutrient signaling and growth control. *Genetics,* 189**,** 1177-201.

MASON, J. S., WILEMAN, T. & CHAPMAN, T. 2018. Lifespan extension without fertility reduction following dietary addition of the autophagy activator Torin1 in Drosophila melanogaster. *PLoS ONE,* 13**,** e0190105.
NAGARAJAN, V. P., M. 2006. *Gene List Venn Diagram* [Online]. Available: http://genevenn.sourceforge.net/ [Accessed].
NISHIDA, K. & SILVER, P. A. 2012. Induction of biogenic magnetization and redox control by a component of the target of rapamycin complex 1 signaling pathway. *PLoS Biol,* 10**,** e1001269.
RALLIS, C., CODLIN, S. & BAHLER, J. 2013. TORC1 signaling inhibition by rapamycin and caffeine affect lifespan, global gene expression, and cell proliferation of fission yeast. *Aging Cell,* 12**,** 563-73.
RALLIS, C., LÓPEZ-MAURY, L., GEORGESCU, T., PANCALDI, V. & BÄHLER, J. 2014. Systematic screen for mutants resistant to TORC1 inhibition in fission yeast reveals genes involved in cellular ageing and growth. *Biology Open,* 3**,** 161-171.
SCHREIBER, K. H., ORTIZ, D., ACADEMIA, E. C., ANIES, A. C., LIAO, C. Y. & KENNEDY, B. K. 2015. Rapamycin-mediated mTORC2 inhibition is determined by the relative expression of FK506-binding proteins. *Aging Cell,* 14**,** 265-73.
SHERTZ, C. A., BASTIDAS, R. J., LI, W., HEITMAN, J. & CARDENAS, M. E. 2010. Conservation, duplication, and loss of the Tor signaling pathway in the fungal kingdom. *BMC Genomics,* 11**,** 510.
SUZUKI, E., EVANS, T., LOWRY, J., TRUONG, L., BELL, D. W., TESTA, J. R. & WALSH, K. 1996. The human GATA-6 gene: structure, chromosomal location, and regulation of expression by tissue-specific and mitogen-responsive signals. *Genomics,* 38**,** 283-90.
THOREEN, C. C., KANG, S. A., CHANG, J. W., LIU, Q., ZHANG, J., GAO, Y., REICHLING, L. J., SIM, T., SABATINI, D. M. & GRAY, N. S. 2009. An ATP-competitive Mammalian Target of Rapamycin Inhibitor Reveals Rapamycin-resistant Functions of mTORC1. *The Journal of Biological Chemistry,* 284**,** 8023-8032.
TROULINAKI, K. & TAVERNARAKIS, N. 2012. Endocytosis and intracellular trafficking contribute to necrotic neurodegeneration in <em>C. elegans</em&gt. *The EMBO Journal,* 31**,** 654.
VEZINA, C., KUDELSKI, A. & SEHGAL, S. N. 1975. Rapamycin (AY-22,989), a new antifungal antibiotic. I. Taxonomy of the producing streptomycete and isolation of the active principle. *J Antibiot (Tokyo),* 28**,** 721-6.
WAGIH, O. & PARTS, L. 2014. gitter: a robust and accurate method for quantification of colony sizes from plate images. *G3 (Bethesda),* 4**,** 547-52.
WANKE, V., CAMERONI, E., UOTILA, A., PICCOLIS, M., URBAN, J., LOEWITH, R. & DE VIRGILIO, C. 2008. Caffeine extends yeast lifespan by targeting TORC1. *Molecular Microbiology,* 69**,** 277-285.
WEISMAN, R. & CHODER, M. 2001. The fission yeast TOR homolog, tor1+, is required for the response to starvation and other stresses via a conserved serine. *J Biol Chem,* 276**,** 7027-32.
XIE, J., WANG, X. & PROUD, C. G. 2016. mTOR inhibitors in cancer therapy. *F1000Research,* 5**,** F1000 Faculty Rev-2078.
YUAN, C., DING, Y., HE, Q., AZZAM, M. M., LU, J. J. & ZOU, X. T. 2015. L-arginine upregulates the gene expression of target of rapamycin signaling pathway and stimulates protein synthesis in chicken intestinal epithelial cells. *Poult Sci,* 94**,** 1043-51.